A REPORT ON

STEADY STATE ANALYSIS OF REDUCED INDIAN POWER SYSTEM

Submitted

In partial fulfilment of the requirement for the award of the degree

Of

MASTER OF TECHNOLOGY

In

ELECTRICAL ENGINEERING

(With specialization in POWER SYSTEMS ENGINEERING)

Submitted by

ARINDAM MITRA

DEPARTMENT OF ELECTRICAL ENGINEERING

INDIAN INSTITUTE OF TECHNOLOGY, ROORKEE

ROORKEE-247667, (INDIA)

MAY, 2016

CANDIDATE'S DECLARATION

I hereby certify that this report which is being presented in the seminar entitled **"STEADY STATE ANALYSIS OF REDUCED INDIAN POWER SYSTEM"** in partial fulfilment of the requirement of award of Degree of **Master of Technology** in **Electrical Engineering** with specialization in ***Power Systems Engineering***, submitted to the Department of Electrical Engineering, Indian Institute of Technology, Roorkee , India is an authentic record of the work carried out during a period from July 2015 to May 2016 under the supervision of **Dr. N. P. Padhy**, Department of Electrical Engineering, Indian Institute of Technology, Roorkee. The matter presented in this report has not been submitted by me for the award of any other degree of this institute or any other institute.

Date : 24/05/2016

Place : Roorkee **(Arindam Mitra)**

CERTIFICATE

This is to certify that the above statement made by the candidate is correct to best of my knowledge.

(Dr. N. P. Padhy)
Professor
Department of Electrical Engineering,
Indian Institute of Technology,
Roorkee-247667, India

ACKNOWLEDGEMENT

I wish to express my sincere gratitude to my respected supervisors **Dr. Narayana Prasad Padhy, Professor,** Department of Electrical Engineering, Indian Institute of Technology Roorkee, for being helpful and a great source of inspiration. His keen interest and constant encouragement gave me the confidence to complete my work. I wish to extend my sincere thanks for his excellent guidance and suggestion for the partial completion of my work.

Also I would like to thank all the faculty members of Electrical Engineering Department, Indian Institute of Technology, Roorkee, for their guidance and support.

My sincere thanks to the Head of the Department, Electrical Engineering Department, Indian Institute of Technology Roorkee, for providing necessary facilities to carry out the dissertation as well the other faculty members of the department are duly acknowledged.

Arindam Mitra

ABSTRACT

Due to ever increasing demand of electrical power along with penetration of renewable energy sources, a proper analysis have to be carried out to determine the effect of increased power transactions through existing transmission network. Although, analysis of power flow of the full model of a power system is preferable in terms of accuracy, it is impractical owing to the large amount of memory, computational complexity and cost involved. As a result, one has to look for an equivalent reduced model which reflects the original system conditions as accurately as possible. The very idea of obtaining a reduced system is to obtain a miniaturized version of the actual system in order to retrieve specific information which should be as accurate as possible in comparison to the information obtained by the actual system. Also, an accurate reduced model decreases the computational complexity, large memory, cost and time associated with the detailed analysis carried out on original network. In literature, there are various types of reduced equivalents available, owing to different circumstances like reactive-active power management, power system calculations, market-pricing etc. The main objective of this article is determination of a reduced model which can be used to represent either the steady state power transactions at the transmission level between different zones (comprising of aggregated generations and loads) or power transactions through critical lines which in turn can be utilized for system planning and market simulations.

This dissertation report involves the implementation of one of the early network reduction technique known Ward's network equivalent and a recent method based on PTDF. Out of these two, the network reduction as per Ward's method focuses on partitioning a large system into three zones as: the zone which retains selected network lines in the reduced model (internal zone), the zone which is of no interest (external zone) and a boundary zone connecting the two before-mentioned zones. This method is suitable only when all the systems of interest are confined in a single area. But for market studies, specific systems can be located anywhere in the actual model and this entails one to adopt means of network reduction based on PTDF (power transfer distribution factors). The method based on PTDF makes use of a dc-flow model. The dc-flow model comprises of linear systems only and thus computational time and memory required are much less as compared to the ac-flow models, which comprise of non-linear system due to which iterative solution has to be conducted. A PTDF matrix acts as the link between powers injected at different locations to the power flowing in different transmission lines and as a result of this, more accurate reduced network equivalents are obtained by reduction of the PTDF matrix. However, models based on PTDF (based on approximations of DC-power flow), because of converting an empirical problem into linear one, yields a linear solution. Difference exists between the empirical solution and the linear one (owing to the difference in problem-solving technique) and considering the practical scenarios, the empirical solutions are more accurate. In this report, steps have been taken to extend the method based on PTDF to yield more accurate power flows i.e. closer to an empirical solution. Finally, the ideas developed in this report are extended to obtain a reduced equivalent model of actual Indian Power System.

TABLE OF CONTENTS

Page

LIST OF TABLES

Page

LIST OF FIGURES

Page

NOMENCLATURE

ac	Alternating current
Bbranch	branch susceptance matrix of order *L-by-N*
Bbus	bus susceptance matrix of order *N-by-N*
Bflow	branch susceptance matrix (*L-by-N) of* the full system
C	node-branch incidence matrix (*L*-by-*N)* of the full system
C_R	node-branch incidence matrix (L_R-by-N_R) of the reduced system
CL	columns of PTDF matrix (representing actual system buses)
D^2	Euclidian norm
diag(x)	Diagonal matrix of branch reactance x
fcm	fuzzy-c-means clustering
G_k	kth injection group
H_R	PTDF matrix with zonal injections and intra-group lines removed
I_{Gi}	output current of generator at bus i
I_{Li}	Load current at bus *i*
k	number of clusters
L	Total lines in the actual system
Le	inter-group lines in the original network
Li	intra-group lines in the original network
L_R	no. of branches in the reduced system
m_{Gi}	no. of generators in group (area) i
m	fuzzy partition matrix exponent
n	no. of buses in the reduced network
N_B	no. of non-slack buses in the full network

Nbranch	no. of designated branches in the system
NR	no. of non-slack buses in the reduced network
Pflow	*L-by-1* branch power flow vector
P_flowr	L_R*-by-1* branch power flow vector
P_{flow}^{int}	intra-zonal power flow
P_{flow}^{ext}	inter-zonal power flow
P_{Gi}	Real power output of a generator at bus *i*
Pinj	bus injection vector (*N*-by-1) of the full system
P_injr	bus injection vector (*NR-by-1*) of the reduced system
P_{Li}	Real power component of a load at bus *i*
PTDF	Power transfer distribution factor
$PTDF_R$	PTDF matrix for the reduced system
Q_{Gi}	Reactive power output of a generator at bus i
Q_{Li}	Reactive power component of a load at bus i
REI	Radial equivalent independent
SSE	Sum of squared errors
TL	Transmission line
v_i	vector of cluster prototypes (centres)
x	branch reactance vector *(L-by-1)* of the full system
x_R	branch reactance vector (L_R*-by-1*)of the reduced system
XB	Xie-Beni index
σ	net deviation
θ	N_B-by-1 vector containing the bus voltage angles of the full system

θij	voltage angle difference between zone *i* and *j*
θ_{flow}	L_R-*by-Le* matrix to sum flows
θ_{inj}	N_R-*by-N* matrix to sum bus injections

CHAPTER 1
INTRODUCTION

1.1 Overview:

Due to ever increasing demand of electrical power along with non-uniform penetration of renewable energy sources, the power transactions through the existing transmission lines is continuously increasing. Thus, a proper analysis have to be carried out to determine the effect on power transactions through transmission network. Although, a steady state analysis of the actual system is preferred, but owing to the vastness of the transmission network, it will be computationally challenging task. So, in order to carry out analysis of power transactions with reduced computational burden, a reduced network equivalent is indispensable. The reduced network equivalent is required to reflect the actual power transactions as accurately as possible.

Depending on the requirement, there are two types of network reduction techniques:

[a] Static Network Reduction [b] Dynamic Network Reduction

The static network reduction, as the name suggests, creates an equivalent reduced model of the actual system, which is meant for static analysis which incorporates factors like planning analysis and power flow calculations which in turn can be used for market analysis.[1]

The dynamic network reduction, on the other hand, helps in the derivation of an equivalent reduced model to take into consideration transient effect, like transient stability analysis of a power system, offline analysis of dynamic stability of a power system having small disturbances etc.[2]

This report focuses on the deriving an equivalent reduced model for carrying out steady state analysis in order to determine the inter-zonal and specific lines power flow, hence, only static network reduction is used.

The main objective of this article is determination of a reduced model which can be used to represent either the steady state power transactions at the transmission level between different zones (comprising of aggregated generations and loads) or power transactions through critical lines which in turn can be utilized for system planning and market simulations. Efforts have been made in the past like Ward's equivalent [3], [4], REI [5], [1] but in all of them, the problem associated is the division of entire system in to namely two or three zones: internal, boundary and external. The internal zone comprises of system of interest, external zone comprises of system to be truncated, and the boundary acts as the link between the two. However, the methods are suitable only when all the systems of interest are confined in a single area. But for market studies, specific systems can be located anywhere in the actual model and this entails one to adopt means of network reduction based on PTDF (power transfer distribution factors) [6]. A PTDF matrix acts as the link between powers injected at different locations to the power flowing in different transmission lines and as a result of this, more accurate reduced network equivalents are obtained [7],[8] by reduction of the PTDF matrix.

1.2 Literature Survey:

There currently exists many types of network reduction methods, out of them, only 3 most used network equivalencing techniques have been stated here:

- ❖ Ward's equivalent (and its variations)
- ❖ REI equivalent (and its variations)
- ❖ Power Transfer Distribution Factors (PTDF)

A brief review of the network reduction methods are given below:

(i) Ward's Equivalent: Previously, the Ward equivalent method was used to derive a reduced model of the actual system. It was introduced by Ward in [3] with some improvements stated given in [9], [10].

The Ward's reduction technique dis-integrates a complete system into three subsystems, namely internal, boundary and external. The subsystem of interest/to be retained is the internal subsystem, whereas the external subsystem, which is of not practical concern for a specific situation, is eliminated by using Gaussian elimination.

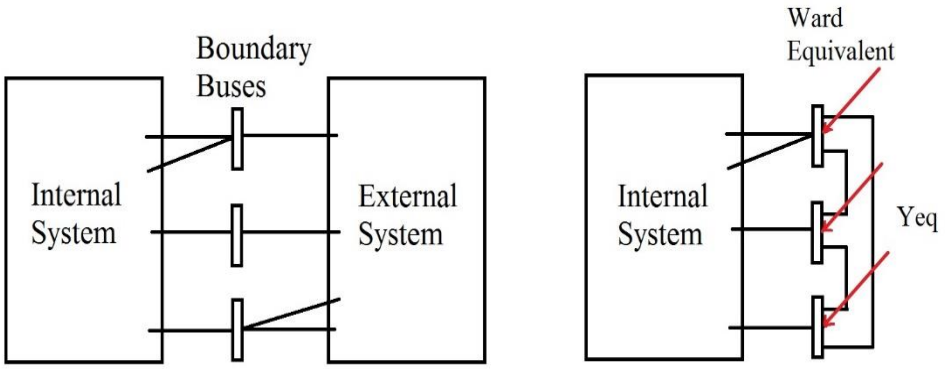

Fig.1.1 Ward's reduction technique [11]

This method, also known as Ward's injection method, converts the power injections at the buses into current injections prior to system reduction, and are converted back to constant power injection after completion of the reduction process.

Limitation in respect to present work: The Ward's equivalent smears or disintegrates the power injection provided by different generators/Loads in order to match the base case power at the boundary buses. Although this result in fairly accurate base case power flow, but it becomes inaccurate while dealing with other than base case power flows as result of new bus injections.

(ii) REI (Radial Equivalent Independent Network): This technique was introduced by P. Dimo [5] with further explanations given in [11]. In this reduction process, the current and power injections present in a group are aggregated and then represented by a fictitious 'REI' node. This fictitious node is used instead of the designated group while constructing the reduced system (figure 1.2(c)).

There are three basic steps in the REI equivalencing process:

1. Power injections from all buses to be aggregated are removed (Figure 1.2.a).

2. An REI network is created and attached to the buses (Figure 1.2.b). Aggregate all the injections SR to the REI node R.

$$S_R = \sum_k S_k \tag{1.1}$$

3. Node G and all buses (k) are eliminated by Gaussian elimination (Figure 1.2.c).

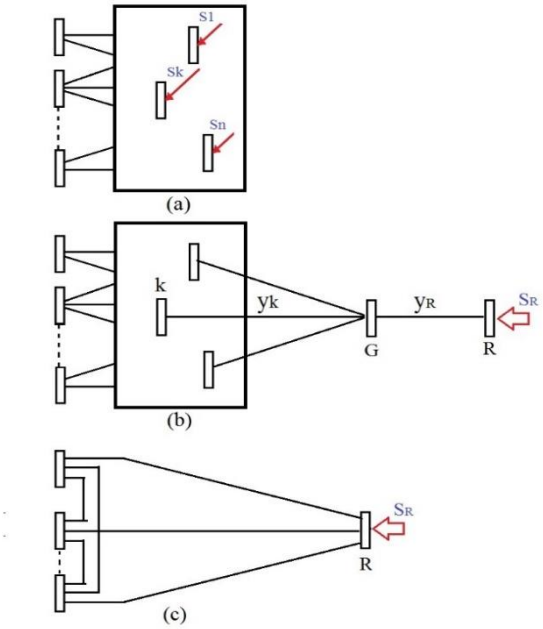

Fig.1.2. REI equivalent, (a) original system with injections to be aggregated (b) attachment of an REI network, (c) resulting REI equivalent after elimination of zero rejection buses [11]

The values of the admittances Y_k and Y_R in the REI network are selected based on a solved load flow of the external system in such a way that the injections into buses k from the REI network are exactly the same as the original injections in the solved load flow. Conventionally, VG (ground voltage) for the base case is set to be zero. Therefore, the values of these admittances should be:

$$y_k = -\frac{S_k^*}{V_k^2} \qquad \text{and} \qquad y_R = -\frac{S_R^*}{V_R^2} \tag{1.2}$$

Limitation in respect to present work: The REI equivalent method has a major drawback, as the equivalent models derived using this method are condition specific and thus yield significant errors in changed operating conditions [11]. More specifically, the admittances of the REI network (equations above) are functions of the operating conditions and as a result the REI equivalent constructed using operating condition A is not the same REI equivalent that would be constructed using operating condition B.

(iii) Power Transfer Distribution Factors: The power transfer distribution factor (PTDF) matrix is a matrix which reflects the relation between line power flows to the power injections at different buses [6], [7],[8]. Once the PTDF matrix is obtained, the power flowing through a transmission line (as a consequence of increment of real power injections at the generator or load buses) can be determined.

$$\textit{Power flow on lines} = \text{PTDF} \times \textit{Power injected at the buses} \tag{1.3}$$

The PTDF matrix calculated from dc-power flow model is most widely used and in this report also, DC-PTDF has been used. Because of the linear nature of dc-flow system, the PTDF matrix can be used to determine power flows in different lines provided that the bus injections are given.

Limitation in respect to present work: Creation of the PTDF matrix is based on DC approximations which convert an empirical problem into a linear one. Because of difference in approach for solution, the empirical and the linear method yield slightly different solution (owing to the difference in problem-solving technique). However, the difference between the linear and empirical solution can be large (i.e. power flows through some of the lines) while handling a large power system.

As the method comprising of PTDF yields the most accurate power flows of all the methods presented above, the work presented in this report is mostly concerned with the application of PTDF and addressing its shortcomings (in terms of accuracy) while dealing with networks ranging from small to very large.

1.3 Report Organization

This report is divided into 5 chapters, which are stated briefly below:

- Chapter 1 gives an overview of the different methods available for creating an equivalent reduced network of the original system and their limitations.
- Chapter 2 presents Ward's Equivalent technique and its implementation on standard IEEE systems.
- Chapter 3 presents basics of Power Transfer Distribution Factors (PTDF)
- Chapter 4 presents a PTDF based network reduction technique and its implementation on standard IEEE system.
- In Chapter 5, a mathematical way of partitioning a system into zones is described which will help in reducing inter-zonal power flow error in different scenarios
- In Chapter 6, a reduced equivalent model of the actual Indian power system (at transmission level) is obtained based on the concepts described in previous chapters.
- In Chapter 7, a brief conclusion and future scope of this work done in this article is presented.

CHAPTER 2

WARD'S EQUIVALENT METHOD

This chapter focus on the implementation of the basic Ward-type equivalent [3], [10]. The basic idea behind this reduction technique is bus elimination by making use of Gaussian elimination method. This chapter is divided into the following sections:

(a) Division of the system into sub-systems

(b) Converting power injections to current injections

(c) Derivation of the system equation

(d) Elimination of the external system

2.1 Division of the system into sub-systems

In the reduction technique introduced by Ward, the first step is to identify the desired and undesired subsystems. Therefore, the complete power system is divided into three parts namely:

- Internal buses
- Boundary buses
- External buses

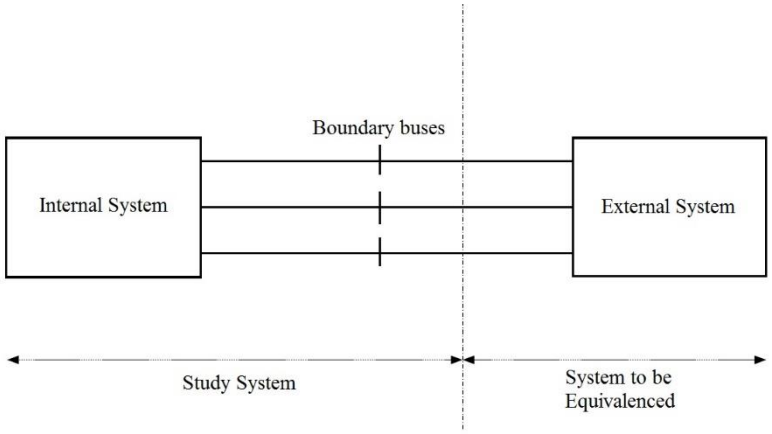

Fig. 2.1. Interconnected power system showing internal, boundary and external system [11]

As shown in fig.2.1, the boundary buses are the only common link between the internal and the external subsystem. The internal subsystem is left intact whereas the external system is equivalenced resulting in a reduced model.

Thus, *our objective is to remove the external buses by replacing them with equivalent injections and lines.*

2.2 Converting power injections to current injections

This method treats the power injections (the external system buses) at the load and the generator buses as constant current quantities.

Consider a bus *i* with a generation characterized by $P_{Gi}+jQ_{Gi}$. The following equation holds,

$$P_{Gi} + jQ_{Gi} = V_i \cdot I_{Gi}^* \tag{2.1}$$

where, P_{Gi} and Q_{Gi} = Real and reactive power at bus i(output of the generator)
V_i = voltage at bus i
I_{Gi} = generator output current at bus i

The generator output current at bus i, in terms of the power injected by the generator at bus i, can be stated as:

$$I_{Gi} = \frac{P_{Gi} - jQ_{Gi}}{V_i^*} \tag{2.2}$$

Similarly, for a load defined by $P_{Li}+jQ_{Li}$, the corresponding load current can be computed as:

$$I_{Li} = \frac{P_{Li} - jQ_{Li}}{V_i^*} \tag{2.3}$$

where, P_{Li} and Q_{Li} = Active and reactive power components of load at bus i
V_i = voltage at bus i
I_{Li} = load current at bus i

Thus, the net current injected at bus i can be stated as:

$$I_i = \sum I_{Gi} - \sum I_{Li} \tag{2.4}$$

where I_i is the net injected current at bus *i*; $\sum I_{Gi}$ and $\sum I_{Li}$ stand for the total generator and load current respectively.

2.3 Derivation of the system equation

In this section, the nodal analysis is used for deriving the system equations, where the external, boundary and internal buses are placed in sequence:

$$\begin{bmatrix} Y_{EE} & Y_{EB} & 0 \\ Y_{BE} & Y_{BB} & Y_{BI} \\ 0 & Y_{IB} & Y_{II} \end{bmatrix} \times \begin{bmatrix} V_E \\ V_B \\ V_I \end{bmatrix} = \begin{bmatrix} I_E \\ I_B \\ I_I \end{bmatrix} \tag{2.5}$$

where,

$Y_{xx}, (x = I, B, E) \rightarrow$ self-admittance of the internal, boundary, or external systems
$Y_{xy}, (x, y = I, B, E) \rightarrow$ mutual-admittance between the internal, boundary, and external systems

$V_x, (x = I, B, E) \rightarrow$ voltage vector of the internal, boundary, or the external system

$I_x, (x = I, B, E) \rightarrow$ current vector of the internal, boundary, or the external system

In (2.5), because of the symmetricity of y bus matrix, we will have:

$$Y_{IB} = Y_{BI}^T \tag{2.6}$$

$$Y_{BE} = Y_{EB}^T \tag{2.7}$$

2.4 Elimination of the external system

As stated in the previous sections, the external subsystem is not required and thus has to equivalenced in order to yield reduced network. Here, this elimination is done by elimination of the external subsystem variables V_E and I_E described in (2.5). It can be represented graphically as follows:

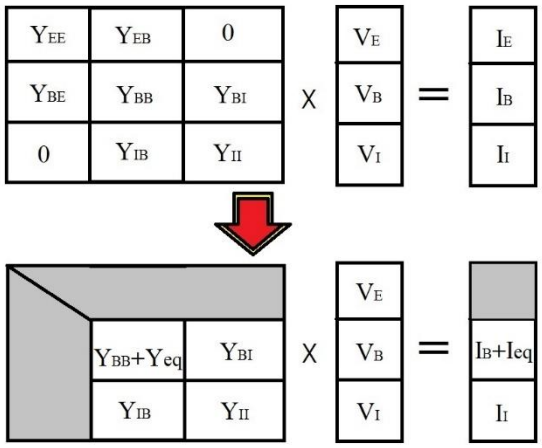

Fig.2.2 Gaussian elimination of V_E and I_E[5]

With the network partitioned as shown in eqn.(2.5), the top partition can be taken out as:

$$Y_{EE}.\, V_E + Y_{EB}.\, V_B = I_E \tag{2.8}$$

Solving for V_E, we get:

$$V_E = Y_{EE}^{-1}.\,(I_E - Y_{EB} V_B) \tag{2.9}$$

Substituting V_E in (2.5), we will get:

$$Y_{BI}.\, V_I + Y_{BB}.\, V_B + Y_{BE}.\, V_E = I_B \tag{2.10}$$

we get:

$$Y_{BI}.\, V_I + Y_{BB}.\, V_B + Y_{BE}.\, Y_{EE}^{-1}.\,(I_E - Y_{EB} V_B) = I_B \tag{2.11}$$

Rearranging the equations, we get:

$$Y_{BI}.V_I + (Y_{BB} - Y_{BE}.Y_{EE}^{-1}.Y_{EB}).V_B = I_B - Y_{BE}.Y_{EE}^{-1}.I_E \quad (2.12)$$

Let , $$Y_{BB}^{'} = (Y_{BB} - Y_{BE}.Y_{EE}^{-1}.Y_{EB}) = Y_{BB} + Y_{eq} \quad (2.13)$$

and $$I_B^{'} = I_B - Y_{BE}.Y_{EE}^{-1}.I_E = I_B + I_{eq} \quad (2.14)$$

Thus, finally we get the system equation as shown in fig 2.2:

$$\begin{bmatrix} Y_{BB}^{'} & Y_{BI} \\ Y_{IB} & Y_{II} \end{bmatrix} \times \begin{bmatrix} V_B \\ V_I \end{bmatrix} = \begin{bmatrix} I_B^{'} \\ I_I \end{bmatrix} \quad (2.15)$$

So, the equivalent admittance and the injection currents are, respectively,

$$Y_{eq} = -Y_{BE}.Y_{EE}^{-1}.Y_{EB} \quad (2.16)$$

and $$I_{eq} = -Y_{BE}.Y_{EE}^{-1}.I_E \quad (2.17)$$

Thus, for equivalencing the external network and then eliminating it, we need the set of equivalent current injections and equivalent admittances values at the boundary bus, the values of which are calculated by eqn.(2.16) and eqn.(2.17). Finally, we will have the reduced equivalent system as shown in fig.(2.3).

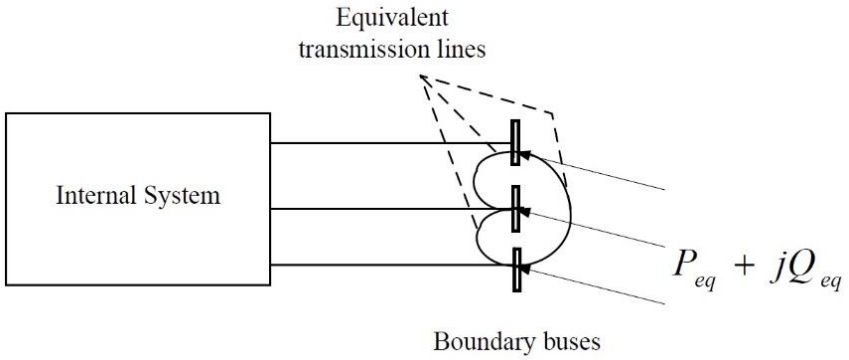

Fig. 2.3 External system equivalencing [11]

The next section discusses the implementation of the Ward's equivalencing method on IEEE 14 and IEEE 30 bus systems.

2.5 Implementation of Ward's method on IEEE 14 and IEEE 30 bus system:

In this section IEEE 14 and IEEE 30 bus system has been reduced to 5 bus and 21 bus system respectively.

(a) IEEE 14 bus to reduced 5 bus system:

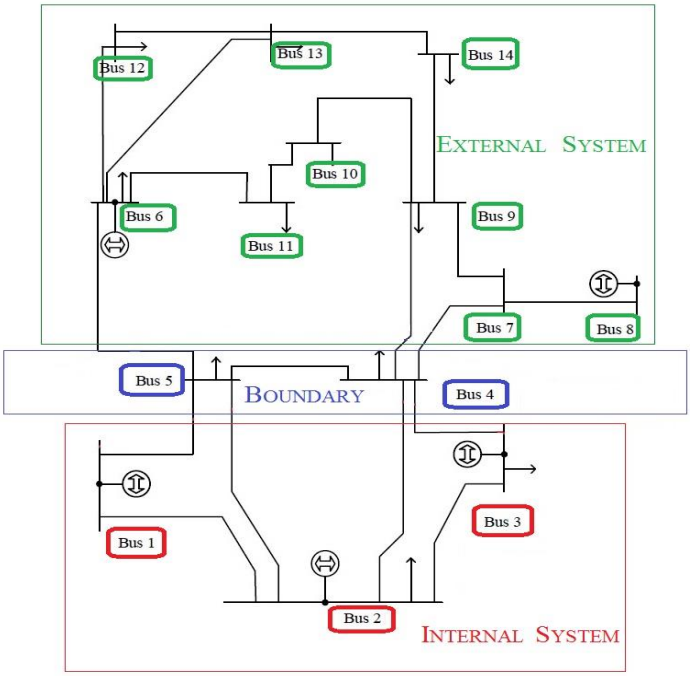

Fig.2.4. IEEE 14 bus system partitioned into 3 regions

As mentioned earlier, the whole system is divided into 3 regions, i.e. internal, boundary & external, internal, boundary & external. As can be seen from the following fig.2.4, that there is no link between the internal and the external buses.

Table 2.1 IEEE 14 bus original System Load-Flow

Bus	Voltage		Pinj (MW)	Qinj (MVAr)
	Mag. (p.u.)	Angle (deg)		
1	1.060	0	237.20	-31.31
2	1.045	-5.182	18.30	-10.60
3	1.046	-14.558	-119.00	-8.76
4	1.029	-10.362	-47.79	-3.90
5	1.036	-8.712	-7.60	-1.60
6	1.055	-12.461	11.20	30.00
7	1.012	-13.497	0	0
8	1.013	-13.520	0	-12.90
9	1.011	-13.663	-29.50	-16.60
10	1.011	-13.739	-9.00	-5.80
11	1.029	-13.220	-3.50	-1.80
12	1.037	-13.393	-6.10	-1.60
13	1.030	-13.483	-13.50	-5.80
14	1.001	-14.647	-14.90	-5.00

Table 2.2 Reduced Equivalent System Load flow

Bus	Voltage		Pinj (MW)	Qinj (MVAr)
	Mag. (p.u.)	Angle (deg)		
1	1.060	0	237.20	-31.31
2	1.045	-5.182	18.30	-10.60
3	1.046	-14.558	-119.00	-8.76
4	1.029	-10.362	-89.28	-33.37
5	1.036	-8.712	-32.18	0.87

It was observed from the above results that the real and reactive power injections at the boundary buses i.e. bus 4 and bus 5 have changed as a result of Equivalencing and it resulted in maintaining the system parameters at the internal buses. (Dark region indicates internal buses).

(a) IEEE 30 bus to reduced 21 bus system:

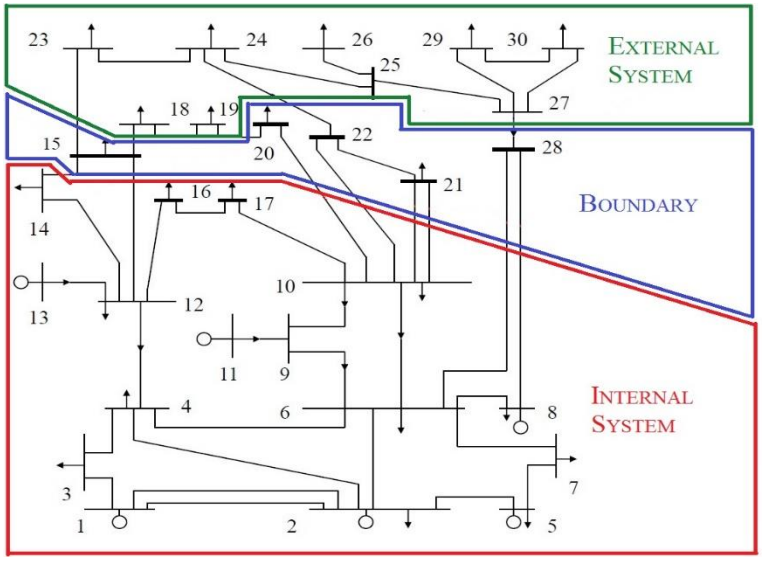

Fig.2.5. IEEE 30 bus system partitioned into 3 regions

Table 2.3 IEEE 30 bus original System Load-Flow

Bus	Voltage		Pinjected (MW)	Qinjected (MVAr)
	Magnitude (p.u.)	Angle (deg)		
1	1.0500	0	238.6700	-29.8400
2	1.0338	-4.9795	35.8600	-5.7000
3	1.0313	-7.9665	-2.4000	-1.2000
4	1.0258	-9.5823	-7.6000	-1.6000
5	1.0058	-13.6010	-69.6400	5.0400
6	1.0218	-11.5030	0	0
7	1.0011	-13.9994	-62.8000	-10.9000
8	1.0230	-12.5685	-45.0000	12.3400
9	1.0461	-13.0409	0	0
10	1.0361	-14.8859	-5.8000	-2.0000
11	1.0913	-11.1688	17.9300	24.0200
12	1.0486	-13.7495	-11.2000	-7.5000
13	1.0883	-12.5608	16.9100	31.0400
14	1.0335	-14.7170	-6.2000	-1.6000
15	1.0283	-14.8674	-8.2000	-2.5000
16	1.0359	-14.5054	-3.5000	-1.8000
17	1.0306	-14.9829	-9.0000	-5.8000
18	1.0187	-15.5811	-3.2000	-0.9000
19	1.0163	-15.8107	-9.5000	-3.4000
20	1.0204	-15.6382	-2.2000	-0.7000
21	1.0231	-15.3595	-17.5000	-11.2000
22	1.0234	-15.3522	0	0

23	1.0165	-15.4200	-3.2000	-1.6000
24	1.0094	-15.8104	-8.7000	-6.7000
25	1.0005	-15.8400	0	0
26	0.9825	-16.2742	-3.5000	-2.3000
27	1.0038	-15.5959	0	0
28	1.0205	-12.1474	0	0
29	0.9835	-16.8750	-2.4000	-0.9000
30	0.9718	-17.7943	-10.6000	-1.9000

Table 2.4 Reduced Equivalent System Load Flow

Bus	**Voltage**		**Pinjected (MW)**	**Qinjected (MVAr)**
	Magnitude (p.u.)	**Angle (deg)**		
1	1.0500	0	238.6700	-29.8400
2	1.0338	-4.9795	35.8600	-5.7000
3	1.0313	-7.9665	-2.4000	-1.2000
4	1.0258	-9.5823	-7.6000	-1.6000
5	1.0058	-13.6010	-69.6400	5.0400
6	1.0218	-11.5030	0	0
7	1.0011	-13.9994	-62.8000	-10.9000
8	1.0230	-12.5685	-45.0000	12.3400
9	1.0461	-13.0409	0	0
10	1.0361	-14.8859	-5.8000	-2.0000
11	1.0913	-11.1688	17.9300	24.0200
12	1.0486	-13.7495	-11.2000	-7.5000
13	1.0883	-12.5608	16.9100	31.0400
14	1.0335	-14.7170	-6.2000	-1.6000
16	1.0359	-14.5054	-3.5000	-1.8000
17	1.0306	-14.9829	-9.0000	-5.8000
15	1.0283	-14.8674	-17.6000	-6.9100
20	1.0204	-15.6382	-11.8500	-4.0400
21	1.0231	-15.3595	-17.5000	-11.2000
22	1.0234	-15.3522	-11.6400	-4.5700
28	1.0205	-12.1474	-10.8300	-7.2300

The shaded rows in Table 2.4 represents the internal buses whereas the unshaded rows represents the boundary buses.

CHAPTER 3

POWER TRANSFER DISTRIBUTION FACTOR

We have seen in the last chapter that though Ward's equivalent is able to conserve base case power flow in the reduced system. But for different operating conditions i.e. as pattern of the generation changes, it is very difficult to assign power injections on the retained bus i.e. on the boundary buses, because the power injection available in the external buses have been distributed among the boundary buses in order to ascertain the equivalent system power flow to be equal to original system's power flow. Thus in order to retain accuracy of power flow in base case as well as non-base case situations, one has to go for PTDF.

3.1 PTDF Matrix

The power transfer distribution factor (PTDF) matrix is matrix which reflects the relation between line power flows to the power injections at different buses. Once the PTDF matrix is obtained, the power flowing through a transmission line (as a consequence of increment of real power injections at the generator or load buses) can be determined. In literature, there are two types of PTDF's:

(a) AC-PTDF

(b) DC-PTDF

An AC-PTDF differs from a DC-PTDF because for creation of DC-PTDF, the assumptions of a dc flow model has to be satisfied. Though AC-PTDF are more accurate than DC-PTDF's, but owing to the non-linear nature of power flows (because of the presence of line losses and reactive power), continuous studies are being carried out to arrive at a proper solution. At present, the PTDF matrix calculated from dc-power flow model is most widely used and in this report also, DC-PTDF has been used.

As compared to AC-PTDF, the DC-PTDF is less accurate, but there are several advantages which outweighs this drawback. The word "dc" in dc power flow comes from the use of old dc network analyzers, used to represent the series reactance as proportional series resistance and the current to represent the corresponding MW flow on the network [6]. The simplest version of dc power flow without any loss compensation, is a further simplification of assuming constant 1 p.u. voltage magnitude. Briefly, the following dc-flow model assumption has to be satisfied:

Assumption 1: Losses are neglected on the branch i.e. resistance is neglected.
$r \approx 0 \rightarrow g_{ij} = 0$ *and* $b_{ij} = -1/x_{ij}$;

Assumption 2: Voltage at the buses are approximate to 1 p.u.
$V_i \approx 1$ for all bus *i;*

Assumption 3: The angle difference across the branch end is small such that
$\sin(\theta_{ij}) \approx \theta_{ij}$

With these simplifications the dc power flow problem is reduced to solving a linear system of equations [6]. This "classical dc" series-reactance model is widely known as the original dc power flow method. It should be also noted that as resistance of a line cannot be "zero", therefore x (line reactance) by r(line resistance) ratio should be greater than or equal to 4 (which is common for transmission lines). Because of the simplification, the dc-flow model becomes a linear system. A graphical representation of shift factors is shown below:

- Say we have a line "L". 1 MW of power is injected at bus A and withdrawn at the reference bus.
- Assume that power flowing through line L in the reference direction is observed to be 0.3 MW, then the shift factor will be 0.3, i.e. 30% [(0.3/1)*100] of the injected power.

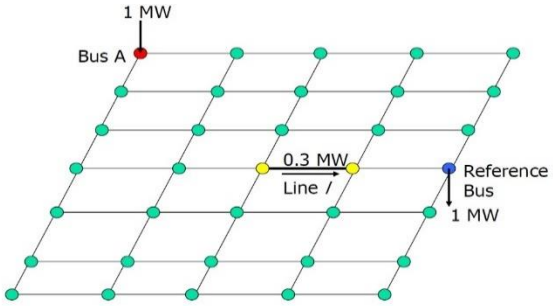

Fig.3.1 Graphical representation of power system with injection at A

- Again, let 1 MW of power is injected at bus B and withdrawn at the reference bus.
- Assume that power flowing through line L in the reference direction is observed to be 0.4 MW, then the shift factor will be 0.4, i.e. 40% [(0.4/1)*100] of the injected power.

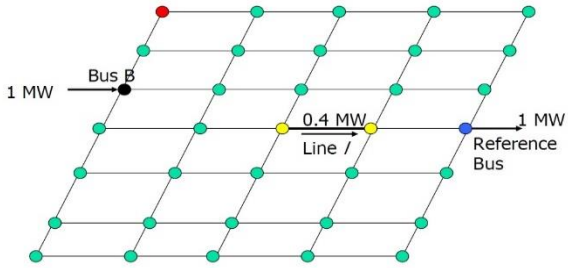

Fig.3.2 Graphical representation of power system with injection at B

- As we have stated before that the dc-flow model is a linear system, thus the law of superposition holds. So, the net power flow through line L will be 0.7 MW (keep in mind the direction of flows)
- In this, one has to select a line and reference direction, and then check the power flow for 1 MW injection at all the buses (except slack /reference bus).

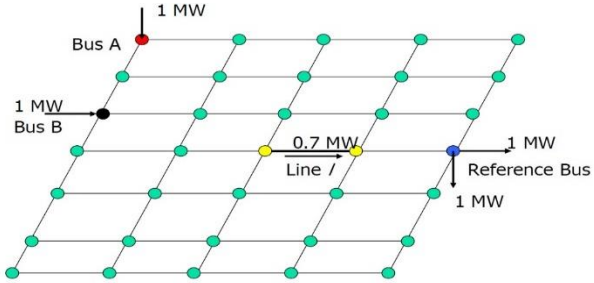

Fig.3.3 Graphical representation of power system with injection at A and B

Thus, because of the linear nature of dc-flow system, the PTDF matrix can be used to determine power flows in different lines provided that the bus injections are given. In the following sections, the theoretical derivation of PTDF has been given, based on which a fast calculating means of PTDF in explained. Finally, a brief overview of significance of PTDF matrix (and its associated factors is given).

3.2 Theoretical Derivation

Prior to [6], PTDF was derived with the help of reactance matrix. The PTDF matrix can be formed as follows:

$$\begin{bmatrix} \Delta P_{flow1} \\ \Delta P_{flow2} \\ \vdots \\ \Delta P_{flowNL} \end{bmatrix}_{NL} = \begin{bmatrix} \rho_{11} & \rho_{12} & \cdots & \rho_{1NB} \\ \rho_{21} & \rho_{22} & \cdots & \rho_{2NB} \\ \vdots & \cdots & \cdots & \vdots \\ \rho_{NL,1} & \rho_{NL,2} & \cdots & \rho_{NL,NB} \end{bmatrix}_{NL\times NB} \begin{bmatrix} \Delta P_1 \\ \Delta P_2 \\ \vdots \\ \Delta P_{NB} \end{bmatrix}_{NB} \tag{3.1}$$

where, NL = no. of TL's in the system
NB = no. of buses in the system
$\Delta P_{flow\ \mathrm{L}}$ = change in the real power flow on line L
ΔP_k = change in the real power injection at bus k

Thus, the elements in the PTDF matrix $\rho_{L,k}$ can be calculated by:

$$\rho_{L,k} = \frac{d\bar{P}_L}{dP_k} \tag{3.2}$$

where, $\bar{\mathrm{P}}_L$ represents the real power flow on the L branch; represents the real power injection at bus$_k$.

As the dc-flow model is a linear system, the bus voltage angles and the power injections at the buses can be linearly related as:

$$P_{inj} = B.\theta \tag{3.3}$$

or

$$\begin{bmatrix} P_1 \\ P_2 \\ \vdots \\ P_{NB} \end{bmatrix}_{NB} = \begin{bmatrix} B_{11} & \cdots & \cdots & B_{1n} \\ \cdots & \cdots & \cdots & \cdots \\ \cdots & \cdots & \cdots & \cdots \\ B_{NB,1} & \cdots & \cdots & \mathrm{B}_{NB,NB} \end{bmatrix}_{NB\times NB} \begin{bmatrix} \theta_1 \\ \theta_2 \\ \vdots \\ \theta_{NB} \end{bmatrix}_{NB}$$

where, $P_{inj} \rightarrow$ Power injection vector with P_i as the injected power at bus i
$\theta \rightarrow$ bus voltage phase angle vector

The elements of the susceptance matrix B are calculated as:

$$B_{ij} = \frac{-1}{x_{ij}} \text{ , } B_{ii} = \sum_{j=1}^{j=NB} \frac{1}{x_{ij}} \tag{3.4}$$

where, $x_{ij} \rightarrow$ reactance of the branch i-j

Thus, matrix *X* (reactance matrix) can be stated as (considering the slack bus as bus 1):

$$X = \begin{bmatrix} 0 & | & \cdots & \cdots & 0_{NB} \\ \cdots & | & & & \\ \cdots & | & B^{-1}_{(NB-1)\times(NB-1)} & & \\ 0_{NB} & | & & & \end{bmatrix} \tag{3.5}$$

here, the first row and column, whose entries are zeros only, belong to the slack bus.
Let bus *i* be connected to bus *j* by branch L, then $\bar{P}_L$ will be:

$$\bar{P}_L = \frac{\theta_i - \theta_j}{x_{ij}} \tag{3.6}$$

Substituting (3.6) into (3.2) yields:

$$\rho_{L,k} = \frac{d\bar{P}_L}{dP_k} = \frac{d}{dP_k}\left(\frac{\theta_i - \theta_j}{x_{ij}}\right) \tag{3.7}$$

This is followed by:

$$\rho_{L,k} = \frac{d}{dP_k}\left(\frac{\theta_i - \theta_j}{x_{ij}}\right) = \frac{1}{x_{ij}}\left(\frac{d\theta_i}{dP_k} - \frac{d\theta_j}{dP_k}\right) = \frac{1}{x_{ij}}(X_{ik} - X_{jk}) \tag{3.8}$$

where, $X_{ik}, X_{jk} \rightarrow ik, jk$ elements extracted from the reactance matrix X, respectively

With the PTDF obtained, the power flow on a transmission line for different generation pattern can be calculated as:

$$\bar{P}_L = \bar{P}_{L\_base} + \Delta\bar{P}_L = \bar{P}_{L\_base} + \sum_{k=1}^{NB} \rho_{L,k}.\Delta P_k \tag{3.9}$$

The short coming of this method is that it require more storage space and time. A direct method of determining the PTDF matrix is given by [7]. From here onwards, the slack bus will be considered as bus/node zero, for both: the reduced equivalent as well as the original system. Alongside, it is assumed that in the following derivations, the slack bus has already been eliminated.

As per dc-power flow, both: the power injection as well as the branch power flow are linearly related to bus voltage angle as:

$$P_{inj} = B_{bus}.\theta \tag{3.10}$$

$$P_{flow} = B_{branch}.\theta \tag{3.11}$$

where, $P_{inj} \rightarrow$ the bus net injection vector $(\mathrm{N}\times 1)$

$P_{flow} \rightarrow$ the branch power flow vector $(\mathrm{L}\times 1)$

$B_{bus} \rightarrow$ representsthe bus susceptance matrix $(\mathrm{N}\times \mathrm{N})$

$B_{branch} \rightarrow$ representsthe branch susceptance matrix $(\mathrm{L}\times \mathrm{N})$

Also, as per definition of PTDF, we have:

$$P_{flow} = PTDF.P_{inj} \tag{3.12}$$

Combining equation (3.10) and (3.11), the power flow in the branches can be defined as:

$$P_{flow} = B_{branch}.B_{bus}^{-1}.P_{inj} \tag{3.13}$$

Comparing (3.12) and (3.13), we get:

$$PTDF = B_{branch}.B_{bus}^{-1} \tag{3.14}$$

On the basis of the line reactance vector x ($L\times 1$) and the node-branch incidence matrix C ($L\times N$), B_{bus} and B_{branch} can be calculated as:

$$B_{bus} = C^{T}.diag(1/x).C \tag{3.15}$$

$$B_{flow} = diag(1/x).C \tag{3.16}$$

From equation (3.14),(3.15) and (3.16), we will have:

$$PTDF = diag(1/x).C.[C^{T}.diag(1/x).C]^{-1} \tag{3.17}$$

Though equation (3.12) states that power flow can be obtained through product of PTDF matrix, but a small error occurs (because of the complexity of the system) between the actual power flow and power flow obtained by equation (3.12). It is also worth mentioning that at transmission level, the line resistance is very small as compared to line reactances, thus, as per the referred articles, line resistance will be neglected (one can also see that equation (3.17) only consists of line reactances).

3.3 Result: PTDF matrix of IEEE 14 bus system

In this section, the PTDF matrix of an IEEE 14 bus system [7] is given (as larger system PTDF matrix cannot be accommodated in available space per page). Also, the actual power flow and calculated power flow are presented side by side. The actual power flows and DC power flows of IEEE-30 bus system is also presented.

(a.1) PTDF of IEEE 14 bus system:

Number of rows = number of TL (transmission lines)
Number of columns = number of buses-slack bus=14-1=13

Table 3.1 PTDF matrix of IEEE 14 bus system

1	2	3	4	5	6	7	8	9	10	11	12	13
-0.8380	-0.7465	-0.6675	-0.6106	-0.6299	-0.6573	-0.6573	-0.6519	-0.6480	-0.6391	-0.6317	-0.6330	-0.6437
-0.1620	-0.2535	-0.3325	-0.3894	-0.3701	-0.3427	-0.3427	-0.3481	-0.3520	-0.3609	-0.3683	-0.3670	-0.3563
0.0273	-0.5320	-0.1514	-0.1031	-0.1195	-0.1427	-0.1427	-0.1382	-0.1348	-0.1273	-0.1210	-0.1221	-0.1311
0.0572	-0.1434	-0.3168	-0.2157	-0.2501	-0.2987	-0.2987	-0.2891	-0.2822	-0.2664	-0.2532	-0.2556	-0.2745
0.0774	-0.0711	-0.1994	-0.2918	-0.2604	-0.2159	-0.2159	-0.2246	-0.2310	-0.2454	-0.2575	-0.2553	-0.2381
0.0273	0.4680	-0.1514	-0.1031	-0.1195	-0.1427	-0.1427	-0.1382	-0.1348	-0.1273	-0.1210	-0.1221	-0.1311
0.0800	0.3071	0.5033	-0.3016	-0.0279	0.3589	0.3589	0.2830	0.2278	0.1021	-0.0034	0.0158	0.1662
0.0029	0.0111	0.0182	-0.0109	-0.2171	-0.6342	-0.6342	-0.4513	-0.4097	-0.3151	-0.2356	-0.2501	-0.3633
0.0017	0.0064	0.0104	-0.0062	-0.1246	-0.1661	-0.1661	-0.2590	-0.2351	-0.1808	-0.1352	-0.1435	-0.2085
-0.0045	-0.0174	-0.0286	0.0171	-0.6584	-0.1997	-0.1997	-0.2897	-0.3552	-0.5041	-0.6292	-0.6065	-0.4282
-0.0027	-0.0105	-0.0172	0.0103	0.2057	-0.1202	-0.1202	-0.1744	-0.2846	-0.5350	0.1757	0.1522	-0.0316
-0.0004	-0.0015	-0.0025	0.0015	0.0302	-0.0177	-0.0177	-0.0256	-0.0157	0.0069	-0.5201	-0.1687	-0.0882
-0.0014	-0.0054	-0.0088	0.0053	0.1057	-0.0618	-0.0618	-0.0896	-0.0549	0.0240	-0.2849	-0.5900	-0.3084
0.0000	0.0000	0.0000	0.0000	-0.0000	0.0000	-1.0000	0.0000	-0.0000	0.0000	0.0000	0.0000	-0.0000
0.0029	0.0111	0.0182	-0.0109	-0.2171	0.3658	0.3658	-0.4513	-0.4097	-0.3151	-0.2356	-0.2501	-0.3633
0.0027	0.0105	0.0172	-0.0103	-0.2057	0.1202	0.1202	0.1744	-0.7154	-0.4650	-0.1757	-0.1522	0.0316
0.0018	0.0069	0.0114	-0.0068	-0.1359	0.0794	0.0794	0.1152	0.0706	-0.0308	-0.1951	-0.2413	-0.6034
0.0027	0.0105	0.0172	-0.0103	-0.2057	0.1202	0.1202	0.1744	0.2846	-0.4650	-0.1757	-0.1522	0.0316
-0.0004	-0.0015	-0.0025	0.0015	0.0302	-0.0177	-0.0177	-0.0256	-0.0157	0.0069	0.4799	-0.1687	-0.0882
-0.0018	-0.0069	-0.0114	0.0068	0.1359	-0.0794	-0.0794	-0.1152	-0.0706	0.0308	0.1951	0.2413	-0.3966

(a.2) Actual power flow and calculated power flow for IEEE 14 bus system (having 14 buses and 20 lines):

Table 3.2 Line power flows for IEEE 14 bus system (actual and using PTDF)

Power by load flow solution	**Power flow by PTDF (PTDF×Pinj)**
148.0542	147.881
70.9458	71.119
69.9627	70.050
55.3351	55.226
41.0564	40.904
-24.2373	-24.150
-61.2739	-62.340
28.3515	28.985
16.2202	16.631
43.1283	42.084
6.883	6.305
7.655	7.545
17.3903	17.034
0	0.000
28.3515	28.985
5.617	6.195
9.4547	9.921
-3.383	-2.805
1.555	1.445
5.4453	4.979

(b.1) Actual power flow and calculated power flow for IEEE 30 bus system (having 30 buses and 41 lines):

Table 3.3. Line power flows for IEEE 30 bus system (actual and using PTDF)

Power by load flow solution	**Power flow by PTDF (PTDF×Pinj)**
147.7788	147.902
73.6612	73.538
45.1558	44.9683
71.2612	71.138
75.4009	75.808
63.0821	62.9858
79.5512	79.5507
5.7609	6.168
57.0391	56.632
41.9954	42.0135
13.307	13.2682
10.9685	11.136
-17.93	-17.93
31.237	31.1982
29.2658	28.9555
-16.91	-16.91
8.1101	8.0496
18.8026	18.6293
8.0631	7.9866
1.9101	1.8496
4.5631	4.4866
6.5443	6.4579
3.3443	3.2579
-6.1557	-6.2421
8.3557	8.4421
4.4369	4.5134
15.912	15.8915
7.7009	7.6872
-1.588	-1.6085
5.9684	5.821
6.1129	6.0787
2.7684	2.621
0.1813	-0.0003
3.5	3.5
-3.3187	-3.5003
-16.3187	-16.5003
6.0623	6.0647
6.9377	6.9353
3.6623	3.6647
-3.0046	-2.9865
19.3233	19.4868

Chapter 4

Network Reduction Using PTDF

This chapter aims at finding a reduced equivalent system by reducing the system's PTDF matrix. As described in the previous chapter, the power flow through the transmission lines can be determined by product of PTDF and power injection vector. Using this property, the inter-zonal power flow in the reduced equivalent of the actual network can be obtained by multiplying the reduced system PTDF with zonal injections. So, first of all, the reduced system PTDF matrix need to be calculated from the actual system PTDF matrix. The following sections deals with two most recent methods for selecting zones, calculating reduced system PTDF, and then ascertaining the equivalent line parameters for the reduced equivalent system.

4.1 Defining the Problem:

4.1.1 Model Specification:

In context of the present work, it is presumed that there are N_B+1 buses (1 stands for the slack bus) in the actual system which are interconnected by L lines. When this actual system is reduced and an equivalent model is obtained, then the reduced system will have N_R+1 buses (1 stands for the slack bus) connected by L_R lines. As the reduced equivalent is considerably smaller than the actual large power system, hence, L and N are substantially greater than L_R and N_R respectively. In order to simplify our analysis, the slack bus is designated as node/bus number 0 (zero; for actual and reduced system).

4.1.2 Topology of the reduced system:

As compared to the previous network reducing methods where external area buses are removed and equivalent power injections are introduced, the network reduction method discussed here explicitly preserve all the buses whether they be loads or generators. This objective is achieved by firstly dividing the actual system into smaller partitions or zones and then algebraically adding all the loads and generations present in a zone. Because of preserving all the generations and loads, the method discussed provides a reduced system equivalent which reflects the inter-zonal power flow (under base and non-base cases) more accurately as compared to other methods. The steps considered are briefly explained below:

a) Let we have the following network :

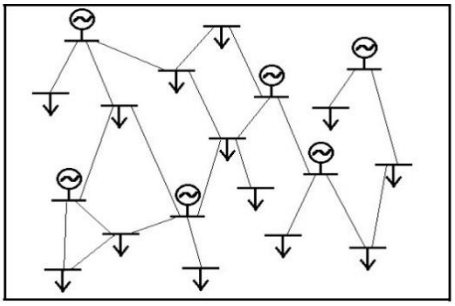

Fig.4.1 Topology of original system

b) Firstly, the actual power network is segregated into different zones (areas). Each of the zones are indicated by an equivalent node/bus.

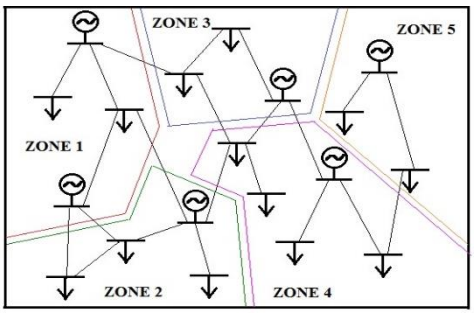

Fig.4.2 System partitioned into desired zones

c) Now, in each of the zones, all the power injections (either by generators or by loads) are added algebraically and the net power injection is represented by the equivalent nodes/buses. The reduced model thus obtained preserves the inter-zonal power transmissions as taking place in the original system as shown in fig.4.3

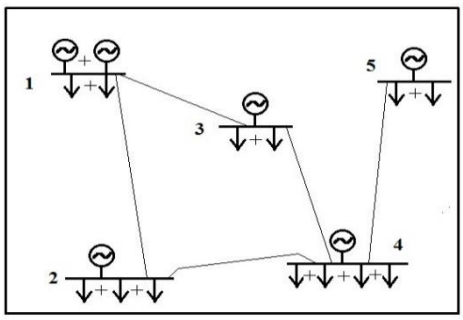

Fig.4.3 Equivalent system

d) Any two zones in the reduced model is connected if and only if at least a single transmission line exists between the buses present in different zones , for example, in fig. 4.3, zone 3 and zone 4 are connected because there exist a transmission line between the buses belonging to these two zones. In the same perspective, zone 3 and zone 5 are not connected in the reduced model as there is no link between any of the buses located in each of the zones.

4.1.3 Problem Formulation

The goal of this development is to determine the reduced system PTDF matrix and arriving at a reduced equivalent model (of the actual power system) consisting of equivalent nodes (representing the zonal injections) interconnected by equivalent lines which reflects the inter-zonal power transactions accurately as the original system under both: base as well as non-base case scenarios. This will be suitable for market studies and can be used as a planning tool to determine the effect of power injections at different locations (by conventional and non-conventional sources) on the existing congested lines.

To achieve the above objective, we have to deduce the reduced system PTDF matrix from the actual system. It is to be noted that the actual system configuration is kept fixed for obtaining

a particular reduced system equivalent as changing the topology will also change the actual system PTDF.

4.2 Problem Solution:

In this section, two different approaches are presented for fulfilling our objective (as stated in the previous section). The solution to each of the method is presented in two parts:

(a) Reduced PTDF Matrix
(b) Equivalent transmission line (TL) reactance

4.2.1 Approach 1 :

(a) Reduced PTDF Matrix ($PTDF_R$):
A PTDF matrix acts as the link between powers injected at different locations to the power flowing in different transmission lines and as a result of this, more accurate reduced network equivalents are obtained by reduction of the PTDF matrix. However, for defining the reduced flow and injection, the groups of buses that are aggregated must be defined [7]. Now, let we have the following defined terms:
Le = total inter-group lines in the reduced system;
Li = total intra-group lines in the reduced system;
(G_1 , G_2 , G_3… G_n) represent injection groups; (P_{Gi}) represent injection; (P_{flow}^{int}) represents the intra-group flow; (P_{flow}^{ext}) represents the inter-group flow.
Separating the inter and intra group flows [7]:

$$P_{flow} = P_f^T \times P_f \times P_{flow} = P^T \times P_{flow}^{ext} \tag{4.1}$$

where, P_f = permutation matrix ordering rows according to inter-zonal groups
Now, the inter-zonal/reduced flow can be obtained by [7]:

$$\begin{aligned} P_{flow\_R} &= \theta_{flow} \times [0^{Le \times Li} \quad I_{Le}] \times P_{sign} \times P_{flow}^{ext} \\ &= \theta_{flow} \times [0^{Le \times Li} \quad I_{Le}] \times P_{sign} \times P_f \times P_{flow} \end{aligned} \tag{4.2}$$

where, P_{flow_R} = inter-zonal power flow

θ_{flow} = $L_R \times L_e$ matrix to sum line flows

P_{sign} = a diagonal matrix of size $L_e \times L_e$ where an element is 1 (if the direction of power flow through a line is same as the inter-group flow) or -1

I_{Le} = identity matrix of size $L_e \times L_e$

Further, we have to aggregate the zonal injections also. So, grouping the power injections, we get:

$$P_{inj} = P_g^T \times P_g \times P_{inj} = P_g^T \times \begin{bmatrix} P_{G1} \\ \vdots \\ P_{Gn} \end{bmatrix} = P_g^T \times P_{injection} \tag{4.3}$$

where, P_g = permutation matrix ordering rows according to injection groups

$P_{injection}$ = Power injection vector re-arranged according to group/zones

So, the zonal injections are given by:

$$P_{inj\_R} = \theta_{inj} \times P_{injection} \tag{4.4}$$

where, θ_{inj} = $N_R \times N_B$ matrix to sum bus injections

As per the definition of $PTDF_R$, we will have the following relation between inter-zonal power flow and zonal power injection:

$$P_{flow\_R} = PTDF_R \times P_{inj\_R} \tag{4.5}$$

Putting values from equation (4.2) and (4.4) in (4.5), we get:

$$\theta_{flow} \times [0^{Le \times Li} \quad I_{Le}] \times P_{sign} \times P_f \times P_{flow} = PTDF_R \times \theta_{inj} \times P_g \times P_{inj} \tag{4.6}$$

Putting value of P_{flow} from equation (3.12), we get [7]:

$$\theta_{flow} \times [0^{Le \times Li} \quad I_{Le}] \times P_{sign} \times P_f \times PTDF \times P_{inj} = PTDF_R \times \theta_{inj} \times P_g \times P_{inj} \tag{4.7}$$

or

$$\theta_{flow} \times [0^{Le \times Li} \quad I_{Le}] \times P_{sign} \times P_f \times PTDF = PTDF_R \times \theta_{inj} \times P_g \tag{4.8}$$

Equation (4.8) is an over determined problem. By applying error minimization process, we get:

$$PTDF_R = \theta_{flow} \times H_R \times \theta_{inj}^T \times W_{injection}^{n \times n} \tag{4.9}$$

where,

$$H_R = [0^{Le \times Li} \quad I_{Le}] \times P_{sign}^{L \times L} \times P_f^{L \times L} \times PTDF^{L \times N} \times (P_g^{N \times N})^T \tag{4.10}$$

and

$$W_{injection}^{n \times n} = (\theta_{inj}^{n \times N} . [\theta_{inj}^{n \times N}]^T)^{-1} \tag{4.11}$$

In the above equations, H_R is the column and row rearranged PTDF matrix corresponding to the flow and the injection groups.

Alongside $PTDF_R$, we also have to determine the reduced node-branch incidence matrix C_T. For a particular system structure, a reduced node-branch incidence matrix C_T is determined as:

$$C_r^{L_R \times N_R} = W_{flow}^{L_R \times L_R} \times \theta_{flow}^{L \times Le} \times C_R \times \theta_{inj}^T \tag{4.12}$$

where,

$$C_R = [0^{Le \times Li} \quad I_{Le}] \times P_{sign}^{L \times L} \times P_f^{L \times L} \times C^{L \times N} \times P_g^T \tag{4.13}$$

$$W_{flow}^{L_R \times L_R} = (\theta_{flow} . [\theta_{flow}]^T)^{-1} \tag{4.14}$$

C represents the node-branch incidence matrix of the original system.

(b) Equivalent transmission line (TL) reactance:

In this section, the reactance of a TL is deduced from the equations of the PTDF matrix. For the actual system, assume that we know the PTDF matrix and the node-branch incidence matrix C, and from using these two, the TL reactance are deduced by using several mathematical properties. From, the previous chapter, we have the following equation:

$$PTDF = diag(1/x).C.[C^T.diag(1/x).C]^{-1} \tag{4.15}$$

where, x is the TL reactance to be deduced. Rearranging equation (4.15), we get:

$$PTDF.C^T.diag(1/x).C = diag(1/x).C \tag{4.16}$$

Let, $PTDF.C^T = A$ and $diag(1/x).C = \lambda$; then equation (4.16) can be written as follows:

$$A.\lambda = \lambda \tag{4.17}$$

Equation (4.17) invokes the mathematical expression where A acts as a *Projection Matrix.*

Also, the one of the properties of *Projection matrix* is inherited by A i.e. A^2=A. A unique feature of a projection matrix is having all its eigen values either 0 or 1. This property of the projection matrix will be utilized here.
As both PTDF and C^T have (N-1) rank, the product $PTDF \times C^T$ will also have (N-1) rank. Out of the total number of eigen values, only the number of eigen values equivalent to the rank of [$diag(1/x).C$] will span the real space of $PTDF \times C^T$. In other words, the eigen value decomposition of $PTDF \times C^T$ yields:

(a) Zero eigen values of which corresponding eigenvectors span the null space of $PTDF \times C^T$
(b)Unity eigen values of which corresponding eigenvectors span the actual solution space of $PTDF \times C^T$.

To estimate the TL reactance *x* from the PTDF matrix, a mathematical approach based on eigen values and eigen vectors has been considered in [7]. By eigen value decomposition of $PTDF \times C^T$, one will obtain only unity or zero values as mentioned above. As the eigen values have unity value constitutes of the solution in the real space, the eigen vectors corresponding to the unity eigen values are considered and stored in new matrix ***Z***. It should be noted that the eigen vectors are not distinctively defined (as the eigen values spanning the real space have the same value i.e. 1), it becomes difficult to calculate the line reactances directly from the PTDF matrix. Alongside, a unit vector 'e' is also present in the real space of ***Z***. The unit vector 'e' has the property to remain unchanged if it is multiplied by $PTDF \times C^T$. This 'e' is included in ***Z*** which generates a new matrix ***Zd*** (=[Z e]). The rank of ***Z*** and ***Zd*** are same.

The next step is to perform a QR factorisation of ***Zd***. The basic goal of the QR decomposition is to *factor* a matrix as a product of two matrices (traditionally called Q,R, hence the name of this factorization). Each matrix has a simple structure which can be further exploited in dealing with linear equations. QR-factorization of the ***Zd*** matrix yields the actual and empty/void

spaces spanned by the matrix as shown below:

$$QR\left\{V^{L\times(N_B-1+ne)}\right\}=\left[Q_1^{L\times(N_B-1)}\quad Q_2^{L\times(L-N_B+1)}\right]\times\begin{bmatrix}R_1^{(N_B-1)\times(N_B-1+ne)}\\0\end{bmatrix} \tag{4.18}$$

where, ne = number of e vectors (here n=1)
Now, the empty space of ***Zd*** (which is same as the null space of *diag(1/x)*C*) is perpendicular to the actual space of ***Zd***. Therefore:

$$Q_2^T\times diag(1/x)\times C=0 \tag{4.19}$$

or $$Q_2^T\times diag(1/x)\times c_j=0,\ \text{ where C} = [c_1, c_2, \ldots\ldots, c_{N-1}] \tag{4.20}$$

Simple linear algebra dictates that:

$$\begin{aligned} Q_2^T\times diag(1/x)\times c_j=0 \ &\leftrightarrow\ Q_2^T\times diag(c_j)\times(1/x)=0\\ &\rightarrow\ \Omega\times(1/x)^{L\times1}=0\end{aligned} \tag{4.21}$$

where,

$$\Omega=\begin{bmatrix}Q_2^T.diag(c_1)\\Q_2^T.diag(c_1)\\\vdots\\Q_2^T.diag(c_{N-1})\end{bmatrix}^{[(L-N+1)L\times L}$$

Although, a trivial solution exists (i.e. 1/x=0); however, such a solution is not feasible as it would mean that all the zones in the reduced system are isolated from each other which, of course, is not a practically feasible solution.
It is interesting to note one of the properties of linear system that if a non-zero constant number is multiplied with all the line reactances in a network, the PTDF matrix will remain unchanged, which can be verified by considering equation (4.21). From equation (4.21), it can be seen that any multiple of (1/x) is also a solution of the equation. However, the scaling of (1/x) cannot be too large or too small, which will lead to very large or very small bus voltage angle which is unrealistic. Hence, a proper value has to be ascertained which is neither too large nor too small. For this purpose, equation(4.21) is modified to:

$$\min_x\ \Omega(1/x)\big|_k,\quad \text{subjected to } \left|\frac{1}{x}\right|_k\geq H(>0) \tag{4.22}$$

where, H represents a small non-negative number. According to [7], a LaGrange function can be formed for the optimization problem:

$$L=y^T\Omega^T\Omega y+\lambda(M-y^Ty) \tag{4.23}$$

where, $y=\left[\frac{1}{x_i}\right]$

An optimality condition says:

$$\frac{dL}{dy}=2\Omega^T\Omega y-2\lambda y=0\ \rightarrow\ (\Omega^T\Omega)y=\lambda y \tag{4.24}$$

As determined in [7], the line susceptance (y) is the eigenvector analogous to the minimum eigenvalue in the absolute value of $\Omega^T\Omega$.
As the $PTDF_R$ and PTDF have same structural properties (i.e. both are having rank equal to one less than number of buses), the reduced system equivalent line reactances can also be deduced by the above mentioned method provided $PTDF_R$ and C_R are already determined.

(c) Algorithm of Approach 1

In this section, the complete work of approach 1 is briefly presented, and by following the steps mentioned here, one can determine the reduced network equivalent as per one's requirement.

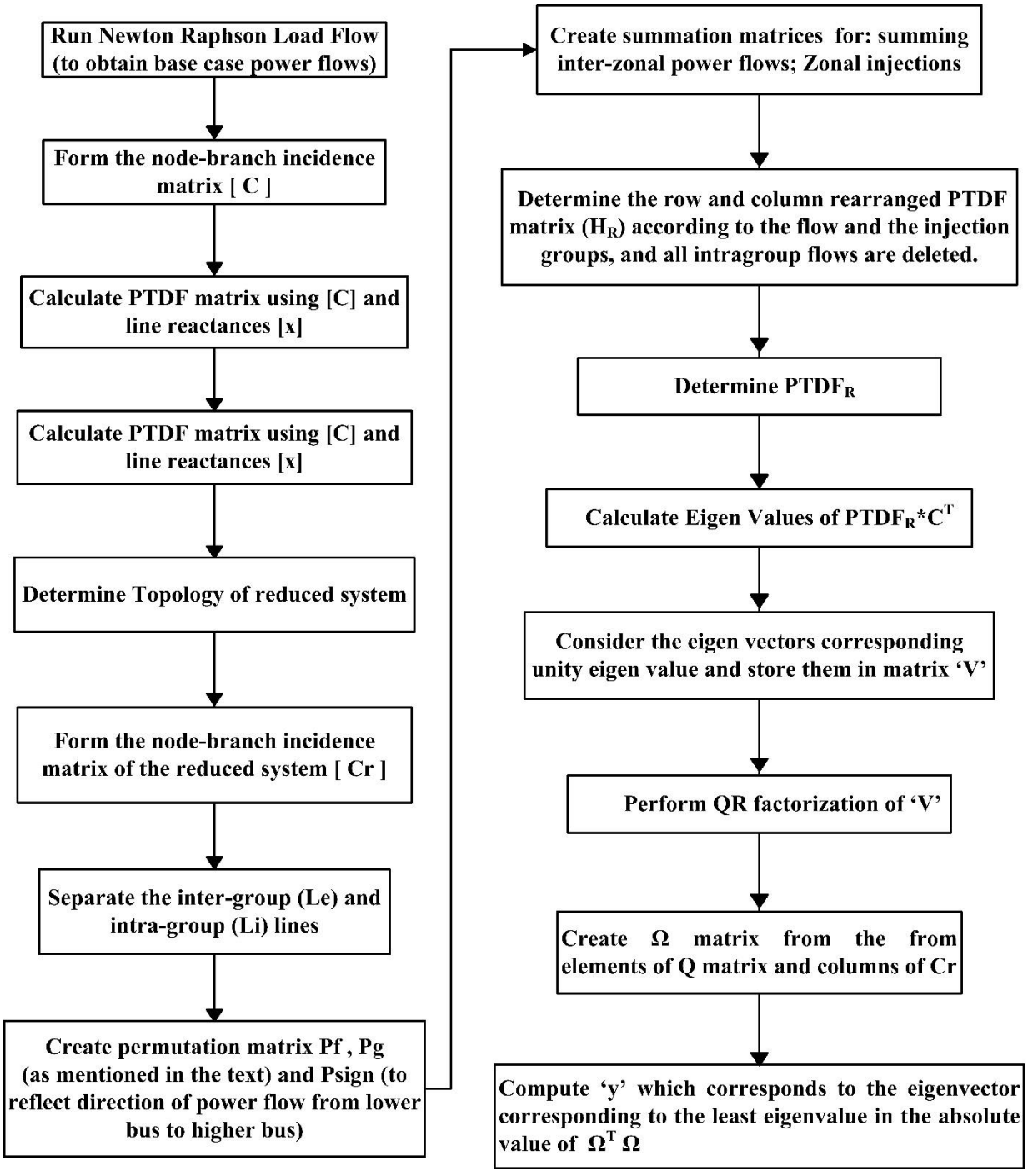

Fig.4.4. Algorithm for determining reduced network equivalent by Approach 1

(d) Results

In this section, a 6 bus test case has been reduced to 4 bus system [7]

(i) 6 bus system reduced to 4 bus system:

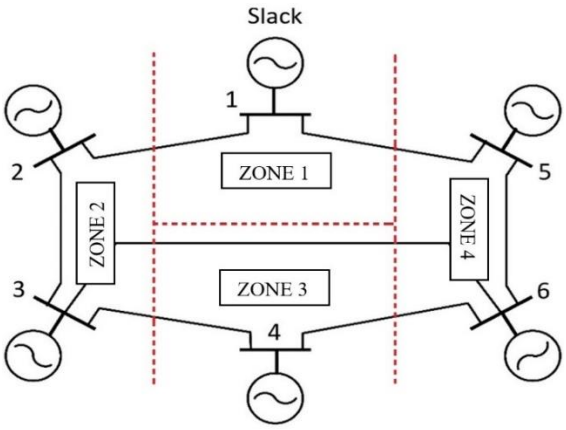

Fig 4.5 Illustrative 6 bus system

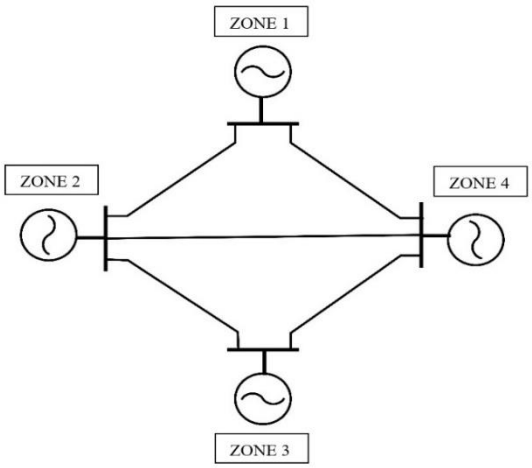

Fig 4.6 Reduced 4 zone system

All the line reactances are 0.1 p.u. (line resistances are 0). The bus injections in fig.4.5. are -5,1,1,1,1,1 (in p.u.) at the buses 1,2,3,4,5 and 6 respectively. Here only sink is the slack bus.

- PTDF matrix of the 6 bus system:

0	-0.7857	-0.5714	-0.5	-0.2143	-0.4286
0	-0.2143	-0.4286	-0.5	-0.7857	-0.5714
0	0.2143	-0.5714	-0.5	-0.2143	-0.4286
0	0.0714	0.1429	-0.5	-0.0714	-0.1429
0	0.1429	0.2857	0	-0.1429	-0.2857
0	0.0714	0.1429	0.5	-0.0714	-0.1429
0	-0.2143	-0.4286	-0.5	0.2143	-0.5714

(PTDF determined matches exactly as stated in [7])

- Node-incidence branch matrix of actual 6 bus system:
  - Slack bus included:

1	-1	0	0	0	0
1	0	0	0	-1	0
0	1	-1	0	0	0
0	0	1	-1	0	0
0	0	1	0	0	-1
0	0	0	1	0	-1
0	0	0	0	1	-1

- Excluding Slack bus:

-1	0	0	0	0
0	0	0	-1	0
1	-1	0	0	0
0	1	-1	0	0
0	1	0	0	-1
0	0	1	0	-1
0	0	0	1	-1

- Injected power at the buses and the power flow in the 6 bus system [7]:

Table 4.1. Injected power and power flows in the actual system

Bus	Injected Power
1	-5
2	1
3	1
4	1
5	1
6	1

From Bus	To Bus	Power Flow
1	2	-2.5
1	5	-2.5
2	3	-1.5
3	4	-0.5
3	6	0
4	6	0.5
5	6	-1.5

(one can multiply the previously stated PTDF matrix with power-injection vector in order to get the power flow vector)
In order to check the authenticity of power flow values, a Newton Raphson load flow was conducted on the 6 bus system to check the power flows. The result are shown in appendix section.

- The reduced system sensitivity matrix $PTDF_R$:

0	-0.6786	-0.5	-0.3214
0	-0.3214	-0.5	-0.6786
0	0.1071	-0.5	-0.1071
0	0.2143	0	-0.2143
0	0.1071	0.5	-0.1071

($PTDF_R$ determined matches exactly as stated in [7])

- Zonal-Power injections(P_injr) and inter-zonal power flow (Pflow_r):

Table 4.2 Injected power and power flows in the reduced system consisting of 4 zones

Zone	Power Injected
I	-5
II	2
III	1
IV	2

Links	Pflow_r = $PTDF_R$*P_injr
I → II	-2.5
I → IV	-2.5
II → III	-0.5
II → IV	0
III → IV	0.5

(Pflow_r obtained is as per [7])

(e) Error associated with Approach 1 and its mitigation:

Though the network reduction worked well, but there is a flaw in the process. Recalling that the input in the 6 bus system was -5,1,1,1,1 and 1 for the buses 1,2,3,4,5 and 6. Taking MVA base as 100 MVA, these bus injections will be -500,100,100,100,100,100.

In order to bring into light the flaw associated with **Approach 1** [7]**,** two non-base case are considered. Among these two non-base cases, the first case has a different set similar power injections at all the buses (except slack) in respect to the already considered power injections above. In the second case a set of dissimilar power injections are considered. Both the cases are dealt with in the next page.

Case (i): A set of similar bus injections are considered as: -750,150,150,150,150 & 150. The PTDF matrix will remain same as there is no change in line parameters. The load flow results obtained is:

Table 4.3 Load flow results of 6 bus system with a set of similar injections

Line FLow and Losses

From Bus	To Bus	P MW	Q MVar	From Bus	To Bus	P MW	Q MVar	Line Loss MW	Line Loss MVar
1	2	-375.000	7.034	2	1	375.000	7.034	0.000	14.067
1	5	-375.000	7.034	5	1	375.000	7.034	0.000	14.067
2	3	-225.000	2.532	3	2	225.000	2.532	0.000	5.063
3	4	-75.000	0.281	4	3	75.000	0.281	0.000	0.563
3	6	0.000	0.000	6	3	-0.000	0.000	0.000	0.000
4	6	75.000	0.281	6	4	-75.000	0.281	0.000	0.563
5	6	-225.000	2.532	6	5	225.000	2.532	0.000	5.063
Total Loss								0.000	39.386

Thus zonal-power injections, inter-zonal power flow and the power flow obtained by product of $PTDF_R$ and P_injr will be:

Table 4.4 Injected Power and Power Flow error in the reduced 4 zone system

Zone	Power Injected
I	-750
II	300
III	150
IV	300

Links	Pflow_r By NR	Pflow_r = $PTDF_R$*P_injr	Error%
I → II	-375	-375	0
I → IV	-375	-375	0
II → III	-75	-75	0
II → IV	0	0	0
III → IV	75	75	0

It can be seen from previous example that the $PTDF_R$ matrix will work nicely.

Case(ii): A set of dissimilar bus injections are considered as: -400,100,200,50,30 and 20 for the bus 1,2,3,4,5 and 6 respectively. The load flow results are given below:

Table 4.5 Load flow results of 6 bus system with a set of dissimilar injections

Line FLow and Losses

From Bus	To Bus	P MW	Q MVar	From Bus	To Bus	P MW	Q MVar	Line Loss MW	Line Loss MVar
1	2	-232.854	2.711	2	1	232.854	2.711	0.000	5.423
1	5	-167.146	1.397	5	1	167.146	1.397	0.000	2.794
2	3	-132.854	0.883	3	2	132.854	0.883	0.000	1.765
3	4	5.715	0.002	4	3	-5.715	0.002	-0.000	0.003
3	6	61.430	0.189	6	3	-61.430	0.189	0.000	0.377
4	6	55.715	0.155	6	4	-55.715	0.155	0.000	0.310
5	6	-137.146	0.940	6	5	137.146	0.940	0.000	1.881
Total Loss								-0.000	12.554

Thus zonal-power injections, inter-zonal power flow and the power flow obtained by product of $PTDF_R$ and P_injr will be:

Table 4.6 Injected Power and Power Flow error in the reduced 4 zone system

Zone	Power Injected
I	-400
II	300
III	50
IV	50

Links	Pflow_r By NR	Pflow_r = $PTDF_R$*P_injr	Error%
I $\rightarrow$ II	-232.5835	-244.64	-5.1837
I $\rightarrow$ IV	-167.4165	-155.36	7.2015
II $\rightarrow$ III	5.8088	1.78	69.3568
II $\rightarrow$ IV	61.6077	53.57	13.0466
III $\rightarrow$ IV	55.8088	51.7857	7.2087

It can be seen now that there is a great difference between inter-zonal power flow and the power flow obtained by product of $PTDF_R$ and P_injr. The cause of this error is the $PTDF_R$ matrix. Recalling equation (4.9), we have:

$$PTDF_R = \theta_{flow} \times H_R \times \theta_{inj}^T \times W_{injection}^{n \times n} \tag{4.9}$$

Here, the term $\theta_{inj}^T \times W_{injection}^{n \times n}$ is responsible for the error. Let $A = \theta_{inj}^T \times W_{injection}^{n \times n}$. The factor A is responsible for representing the participation of different bus injections re-arranged in zonal groups. The **rows of A** denotes the buses in zonal groups and **columns of A** denotes the zones.

Going back to the example, the factor A is:

$$\begin{bmatrix} 1 & 0 & 0 & 0 \\ 0 & 0.5 & 0 & 0 \\ 0 & 0.5 & 0 & 0 \\ 0 & 0 & 1 & 0 \\ 0 & 0 & 0 & 0.5 \\ 0 & 0 & 0 & 0.5 \end{bmatrix}$$

(i) The first row represent participation of bus 1 in **zone I**. As **zone I** only comprises of bus 1, so, the participation factor of bus 1 is **1.**

(ii) The second and third row represent participation of bus 2 and bus 3 in **zone II**. As **zone II** comprises of two buses, therefore, the participation factor of each of the bus is **0.5**

(iii) The first row represent participation of bus 4 in **zone III**. Again,as **zone III** only comprises of bus 4, so, the participation factor of bus 4 is **1.**

(iv) The fifth and sixth row represent participation of bus 5 and bus 6 in **zone IV**. As **zone IV** comprises of two buses, therefore, the participation factor of each of the bus is **0.5**

Therefore, the $PTDF_R$ matrix comprising **A** works fine when all the bus injections are same, but in case the bus injections are changed, errors occurs while using $PTDF_R$ matrix. So, in case of have different bus injections, we have to construct **A qualitatively rather than quantitatively.** By this statement we mean that, instead of giving **equal weightage to the bus injections in a zone, weightage to a bus should be given as per the contribution of the bus injection in the zonal injection.** In this way, $PTDF_R$ can be made more accurate.

Now, assume that we have **A** ($= \theta_{inj}^{T} \times W_{injection}^{n \times n}$) as:

1	0	0	0
0	0.333	0	0
0	0.667	0	0
0	0	1	0
0	0	0	0.6
0	0	0	0.4

Then, the new $PTDF_R$ obtained would be:

Old $PTDF_R$

0	-0.6786	-0.5	-0.3214
0	-0.3214	-0.5	-0.6786
0	0.1071	-0.5	-0.1071
0	0.2143	0	-0.2143
0	0.1071	0.5	-0.1071

New $PTDF_R$

0	-0.6428	-0.5	-0.3
0	-0.3572	-0.5	-0.7
0	0.119	-0.5	-0.1
0	0.2381	0	-0.2
0	0.119	0.5	-0.1

- Base Case: Determining the new power flow from the new $PTDF_R$ we get:

Table 4.7 Power Flows in the reduced 4 zone system (base case) with new $PTDF_R$

Inter-Links	Pflow_r By NR	old $PTDF_R \times P_{inj}$	new $PTDF_R \times P_{inj}$
I $\rightarrow$ II	-232.5835	-244.6429	-232.8550
I $\rightarrow$ IV	-167.4165	-155.3571	-167.1450
II $\rightarrow$ III	5.8088	1.7857	5.7150
II $\rightarrow$ IV	61.6077	53.5714	61.4300
III $\rightarrow$ IV	55.8088	51.7857	55.7150

- Non-base case: A load of 30 MW and 50 MW are introduced at bus 4 and bus 5 respectively. So, in this case bus 5 also acts as a sink i.e. withdrawing power (as P_{G5}-P_{L5}=30-50=-20) from the network along with the slack. The inter-zonal power flows are:

Table 4.8 Power Flows in the reduced 4 zone system (non-base case) with new $PTDF_R$

Inter-Links	Pflow_r By NR	old $PTDF_R \times P_{inj}$	new $PTDF_R \times P_{inj}$
I $\rightarrow$ II	-206.922	-213.571	-202.857
I $\rightarrow$ IV	-113.078	-106.428	-117.142
II $\rightarrow$ III	24.371	22.142	25.714
II $\rightarrow$ IV	68.706	64.285	71.428
III $\rightarrow$ IV	44.371	42.142	45.714

So, finally we can say that in order to improve the power flow for base case as well as non-base cases, we have to give proper weightage to different buses in **A** ($= \theta_{inj}^{T} \times W_{injection}^{n \times n}$).
In order to avoid the bus injection weightage problem as well as to simplify our calculations, we have to make use of **Approach 2** as discusses in the next section.

4.2.2 Approach 2:

(a) Reduced PTDF Matrix ($PTDF_R$):

In this method, the reduced system sensitivity matrix $PTDF_R$ is determined by exploiting the mathematical relation between the system PTDF matrix and the line reactances [8]. Likewise **Approach 1,** proper matrices has to be constructed in order to obtain zonal injections and zonal flows corresponding to bus injections and line power flows respectively.

In order to obtain the zonal injections from the actual system bus injections, a matrix called *pieg* has to be created such that:

$$(P_{inj})_R = pieg * P_{inj} \tag{4.25}$$

The matrix *pieg* is an N_R-by-N matrix and consists of only 1's and 0's:

- *pieg*(i,j) = 1, if **bus i** in the actual system belongs to **zone j**
- *pieg*(i,j) = 0, if **bus i** in the actual system does not belong to **zone j**

Also, in order to determine the inter-zonal power flows from the actual system line power flows, a matrix called ***pieflow*** is created as:

$$(P_{flow})_R = pieflow * P_{flow} \tag{4.26}$$

The matrix *pieflow* is an N_L-by-L matrix and consists of only 1's and 0's such that an element of pieflow is 1 if and only if the buses present at both the ends of a line in the original system exists in two different zones in the reduced system.

A new matrix β is developed as follows:

$$\beta = pieflow * \text{PTDF} * \text{diag}\,(P_{inj}) * (pieg)^{T} \tag{4.27}$$

where,

$$\text{diag}\,(P_{inj}) = \begin{bmatrix} P_{inj}^{(1)} & 0 & \cdots & 0 \\ 0 & P_{inj}^{(2)} & \cdots & 0 \\ \vdots & & \ddots & \\ 0 & 0 & \cdots & P_{inj}^{(N)} \end{bmatrix}$$

μ is an L_R-by- N_R matrix in which each of the elements depicts the corresponding zone's contribution to the inter-zonal power flows. For example, $\mu^{(2,6)}$ denotes the contribution of zone 2 power injections to the 6th inter-zonal power flow [8]. Mathematically:

$$P_{flow}^{\text{inter-zonal}} = \begin{bmatrix} \sum_{j=1}^{N_R} \beta^{(1,j)} \\ \sum_{j=1}^{N_R} \beta^{(2,j)} \\ \vdots \\ \sum_{j=1}^{N_R} \beta^{(L_R,j)} \end{bmatrix}_{L_R \times N_R} = \beta \tag{4.28}$$

Keeping in the mind the elements and order of matrix β, eqn. (4.5) can be represented as:

$$\beta = \text{PTDF}_R * \text{diag}\,(P_{inj})_R \tag{4.29}$$

Eqn. (4.25), (4.27) and (4.29) considered together yields:

$$\beta = \text{PTDF}_R * \text{diag}\,(pieg*P_{inj}) = pieflow * \text{PTDF} * \text{diag}\,(P_{inj}) * (pieg)^{T} \tag{4.30}$$

From the above equation, the sensitivity matrix PTDF_R for the reduced system can be determined as:

$$\text{PTDF}_R = pieflow * \text{PTDF} * \text{diag}\,(P_{inj}) * (pieg)^{T} * [\text{diag}\,(pieg*P_{inj})]^{-1} \tag{4.31}$$

The calculation of PTDF_R as described in this approach is more accurate as well as computationally efficient with respect to reduced sensitivity matrix as described in **Approach 1.** The reason for this is explained in section 4.4.

(b) Equivalent transmission line (TL) reactance

In this section, the equivalent reactances of the reduced model are determined using PTDF_R. Going back to the actual system, the relation between the transmission line reactances (x) and PTDF matrix is shown in eqn. (4.15) above as:

$$PTDF = diag(1/x).C.[C^{T}.diag(1/x).C]^{-1}$$

Similarly, the relation between the $PTDF_R$ matrix and the line reactances of the reduced system (x_R) can be written as:

$$PTDF_R = diag(1/x_R).C_R.[C_R^T.diag(1/x_R).C_R]^{-1} \quad (4.32)$$

Here, C_R is the node-branch incidence matrix of the reduced equivalent system which is based on the structure of the reduced system.
Now, as shown in eqn. (4.16), by rearranging above equation, we will get:

$$PTDF_R.C_R^T.diag(1/x_R).C_R = diag(1/x_R).C_R \quad (4.33)$$

On further solving, we will get:

$$[PTDF_R.C_R^T - I].diag(1/x_R).C_R = 0 \quad (4.34)$$

Again, as in eqn. (4.20), the matrix C_R can be considered as $C_R = c_i = [c_1, c_2, \ldots\ldots, c_{N_R-1}]$, where c_1, c_2… etc. denotes the column vectors of C_R. Therefore:

$$[PTDF_R.C_R^T - I].diag(1/x_R).c_i = 0 \quad (\text{for } i=1,2,\ldots, N_R) \quad (4.35)$$

As per the rules of linear algebra:

$$\begin{aligned} &[PTDF_R.C_R^T - I].diag(1/x_R).c_i = 0 \\ \leftrightarrow\ &[PTDF_R.C_R^T - I].diag(c_i).(1/x_R) = 0 \end{aligned} \quad (4.36)$$

From now on, $[PTDF_R.C_R^T - I].diag(c_i)$ is considered as Δ, thus :

$$\Delta.(1/x_R) = 0 \quad (4.37)$$

where

$$\Delta = \begin{bmatrix} (PTDF_R.C_R^T - I).diag(c_1) \\ (PTDF_R.C_R^T - I).diag(c_1) \\ (PTDF_R.C_R^T - I).diag(c_1) \\ \vdots \\ (PTDF_R.C_R^T - I).diag(c_{N_R}) \end{bmatrix}_{L_R \times N_R} \quad (4.38)$$

For equation (4.37), like approach 1, a trivial solution exists i.e. $(1/x_R) = 0$; however, such a solution is not feasible as it would mean that all the zones in the reduced system are isolated from each other which, of course, is not a practically feasible solution. In order to get a viable solution for equation (4.37), we need to get a non-zero and positive term on the right hand side of equation (4.37) and then by solving for a system of linear equation, we can obtain the reduced system line reactances. Alongside, it should be noted that the product of the reduced system line reactances with the same non-zero constant number will yield the same PTDF matrix. The non-zero positive number to be considered on the right hand side can considered

as scaling factor for the reduced system line reactances. However, the scaling factor cannot be too large or too small, which will lead to very large or very small bus voltage angle which is unrealistic. Hence, a proper constraint has to be considered which is neither too large nor too small. A reasonable constraint can be acquired by considering the relationship between power flow, bus voltage angles and the line reactances. Consider that the average angle in the zones, say "a" and "b" , is θ_a and θ_b. As per DC power flows, if zones "a" and "b" are connected by "k^{th}" line, we will have:

$$P_{flow\ a\to b} = \frac{\theta_a - \theta_b}{x_R^{(k)}} \tag{4.39}$$

or

$$\frac{1}{x_R^{(k)}} = \frac{P_{flow\ a\to b}}{\theta_a - \theta_b} \tag{4.40}$$

Here, $P_{flow\ a\to b}$ is the base case power flow between zones *a* and *b*.

The left hand side factor can be taken as the required constraint to be augmented in the Δ matrix of equation (4.37) and thus help in the determination of a feasible solution. Mathematically:

$$\Delta^* . \begin{bmatrix} 1 \\ \overline{x_R^{(k)}} \end{bmatrix} = \begin{bmatrix} N_k \\ \Delta \end{bmatrix} . \begin{bmatrix} 1 \\ \overline{x_R^{(k)}} \end{bmatrix} = \begin{bmatrix} \dfrac{P_{flow\ a\to b}}{\theta_a - \theta_b} \\ 0 \end{bmatrix} \tag{4.41}$$

where N_k is a 1-by-L_R matrix with all the elements being zero except the *k*th element.
The solution to equation (4.41) can be easily determined as:

$$\begin{bmatrix} 1 \\ \overline{x_R^{(k)}} \end{bmatrix} = \left[(\Delta^*)^T . \Delta \right]^{-1} . (\Delta^*)^T . \begin{bmatrix} \dfrac{P_{flow\ a\to b}}{\theta_a - \theta_b} \\ 0 \end{bmatrix} \tag{4.42}$$

On solving equation (4.42), one can obtain the reduced system line reactances. The method for calculation of line reaction in **approach 2 [8]** is faster than **approach 1 [7]** which requires an eigen value decomposition, selecting the eigen vectors in solution space, QR factorization and solution to a complex optimization problem.

(c) Algorithm of Approach 2

In this section, the complete work presented in approach 2 is briefly presented, and by following the steps mentioned here, one can determine the reduced network equivalent as per one's requirement.

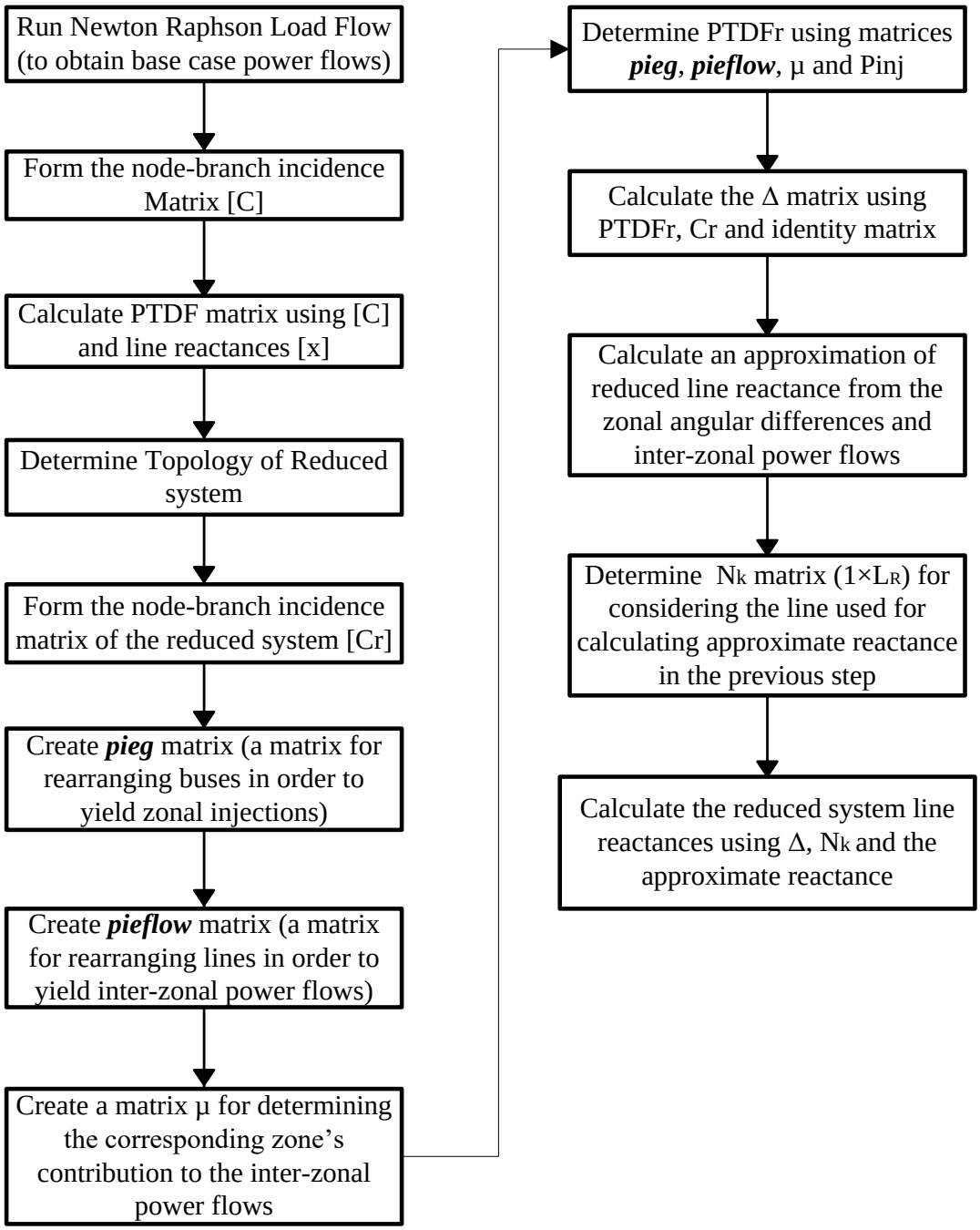

Fig.4.7. Algorithm for determining reduced network equivalent by Approach 2

(d) Implementation on 6 bus test case and IEEE 14 bus system:

In this section, the following two systems are presented:

(i) 6 bus system reduced to 4 bus system [7], [8]

(ii) IEEE 14 bus reduced to 8 bus system

The 6 bust test case is the same as considered in approach 1.

(i) 6 bus system reduced to 4 bus system:

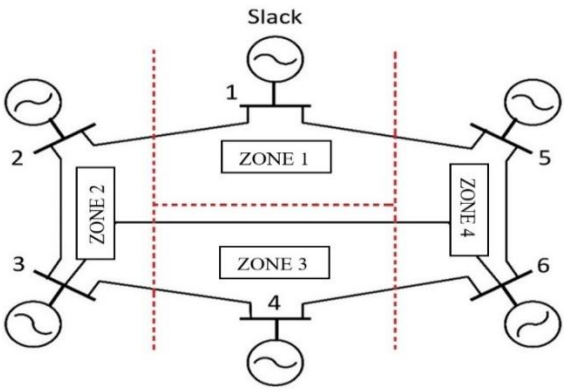

Fig 4.8 Illustrative 6 bus system

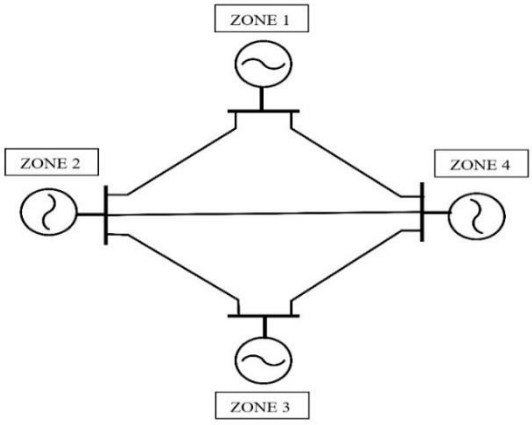

Fig 4.9 Reduced 4 zone system

The line reactances, node-incidence branch matrix and the PTDF matrix are same as stated in the result section of approach 1. As we have stated previously that approach 2 is superior as compared to approach 1, we will proceed directly with the set of dissimilar power injections i.e. -400,100,200,50,30 and 20 for the bus 1,2,3,4,5 and 6 respectively.

- The reduced system sensitivity matrix $PTDF_R$:

0	-0.6429	-0.5	-0.3
0	-0.3571	-0.5	-0.7
0	0.119	-0.5	-0.1
0	0.2381	0	-0.2
0	0.119	0.5	-0.1

(PTDFr is same as [8])

- The injected power and power flows are given in Table 4.9.

Table 4.9 Injected power and power flows in the reduced system consisting of 4 zones

Zone	Power Injected
I	-400
II	300
III	50
IV	50

Links	Pflow_r By NR	Pflow_r = $PTDF_R$*P_injr
I → II	-232.5835	-232.8571
I → IV	-167.4165	-167.1429
II → III	5.8088	5.7143
II → IV	61.6077	61.4286
III → IV	55.8088	55.7143

(Pflow_r is same as in [8])

It can be seen from Table X. that the reduced system inter-zonal power flows are much more accurate that approach 1.

(e) Error associated with Approach 2 and its mitigation:

It is to be understood that the creation of the PTDF matrix is based on DC approximations which convert an empirical problem into a linear one. Because of difference in approach for solution, the empirical and the linear method yield slightly different solution (owing to the difference in problem-solving technique). However, the difference between the linear and empirical solution can be large (i.e. power flows through some of the lines) while handling a large power system. As an empirically obtained solution is closer to an actual one, steps can be taken to fine-tune the line reactances of the reduced system which will yield solution closer to an empirical one for both: base case as well as non-base case operations. For fine-tuning the reactances, a term to be called as "**correction factor [CF]**", has to determined. The CF is the contribution of this article.

In order to clearly view the difference between the linear solution (DC power flow solution) and the empirical solution (AC power flow solution), the corresponding power flows are shown in Table. XI. As stated above, Table. XI. represents the difference in power flows in the two cases: when the PTDF matrix is multiplied to the power injection vector (DC power flow solution) and when a Newton-Raphson load flow is done with all initial bus voltage and angles as 1 p.u. and 0 respectively.

Table 4.10 Power flows obtained by PTDF and NR method on 6 bus test case with same initial conditions and line parameters

Inter-links	***Power Flow (PTDF*Pinj)* [8]**	***Power Flow (NR method)***
1-2	-232.857	-232.584
1-5	-167.142	-167.417
2-3	-132.857	-132.583
3-4	5.714	5.808
3-6	61.428	61.607
4-6	55.714	55.808
5-6	-137.142	-137.416

This comparison is shown just to indicate the difference in power flows even in the actual system. This difference is natural as the solutions are obtained using linear and empirical methods respectively. Though the error is very small (as system used is very small), it tends to increase when we go for higher systems. However, this error can be reduced by using **CF.**

The idea behind CF is to fine-tune the reduced system reactance in order to obtain solution closer to an empirical one. It has to be kept in mind that we are dealing with a linear method i.e. DC power flow method. Consider a linear relationship: say voltage and current which are linearly related to each other by R (V=I*R or I=V*Y). Suppose, we get a current I_1 for a voltage V_1. Now, if we have the same voltage V_1 but we want to get a current I_2, then by fine-tuning

the resistance R, our aim can be accomplished. The above case only represented a linear equation consisting of a single variable. For a larger system, we will have multiple voltages, currents and resistances (i.e. a linear equation in *n*-variables). The existence of solution in such a case can be ascertained by determining the eigen values. Likewise I_1 and I_2, difference exists between the empirical solution and DC power flow solution. Hence, if we fine tune the reactances (used for calculating DC power flow) by a proper factor, then with the fine-tuned reactances we can have a system which yields power flow closer to an empirical solution.

Coming back to our problem, it has been stated [7] that the eigen values (for a practically possible system) of PTDF*C^T will consists of:

- (N_B-1) : ones (as rank of PTDF*C^T is N_B-1)
- L_B-(N_B-1) : zeros.

This check is also valid for the reduced system. If this condition is violated by the reduced system, then such an equivalent system is erroneous. By experimenting with smaller and larger systems, it has been ascertained that:

- Eigen values of (for PTDFr*Cr^T) is either 0 or 1 only if the incoming power at a bus is equal to outgoing power.

Hence, any factor cannot be used to fine-tune the reactances (otherwise eigen values will be something else than only being 0 and 1). But if the CF is mathematically determined as:

$$[CF] = \frac{[P_{\text{flow}}^{\text{inter-zonal}}]\Big|_{NR}}{[PTDF_R] \times [(P_{\text{inj}})_R]} \tag{4.43}$$

and using the CF, the new system susceptance is calculated from the reduced system susceptance (*sus*) obtained in equation (4.42) as:

$$sus_{New} = sus \times CF \tag{4.44}$$

Then, the new PTDFr matrix (called as PTDFrN matrix) can be obtained as:

$$PTDF_R N = diag\left(SUS_{New}\right).C_R.\left[C_R^T.diag\left(SUS_{New}\right).C_R\right]^{-1} \tag{4.45}$$

Only the eigen values 0 and 1 have been obtained for PTDFrN*Cr^T. It should be noted that the use of CF holds true only if:

- System is linear
- The physical structure of the system remains same i.e. no lines have been added or removed from the existing system (as such will chance the PTDF matrix of the original system itself)

From now on for the reduced system, we will be having:

- DC_reac: reactance obtained by [8] i.e. (1/*sus*) or x_R
- AC_reac: reactance obtained by (1 / sus_{New})

This use of **CF** is encouraged as the actual power flow results in a power system are more accurately represented by solutions obtained by empirical methods (which will make use of the equivalent reduced system reactances). In [8], the inter-zonal power flow error is zero and it is

correct in the sense that the results are compared to a DC power flow solution. In order to see the effect of CF, for the 6 bus test case, following three cases are considered. At this point, it should be noted that, along with the utilization of CF, system partitioning also plays a very important role in order to yield accurate power flows for base case as well as non-base case scenarios. Due to this, system partitioning has to be performed by utilizing proper mathematical tools. Such mathematical tools mainly comprises of clustering algorithms.

(i) Base case:

Table 4.11 Inter-zonal power flows at base case

Inter-link between zones	***Power Flow in Original System (By NR)***	***Pflowr with DC_reac* [8]**	***Pflowr with AC_reac***
1-2	-232.584	-232.728	-232.481
1-4	-167.417	-167.272	-167.519
2-3	5.8088	5.7706	5.8276
2-4	61.6077	61.5009	61.6915
3-4	55.8088	55.7706	55.8276
Avg. Error		0.2097	0.1198

(ii) Non-base case (all injection values are uniformly increased by 10%):

Table 4.12 Inter-zonal power flows at non-base case

Inter-link between zones	***Power Flow in Original System (By NR)***	***Pflowr with DC_reac* [8]**	***Pflowr with AC_reac***
1-2	-255.777	-255.985	-255.701
1-4	-184.223	-184.016	-184.299
2-3	6.4121	6.3378	6.4195
2-4	67.8109	67.6776	67.8792
3-4	61.4121	61.3378	61.4195
Avg. Error		0.3340	0.0598

(iii) Non-base case (all injection values are non-uniformly increased by 10%):

Table 4.13 Inter-zonal power flows at non-base case

Inter-link between zones	***Power Flow in Original System (By NR)***	***Pflowr with DC_reac* [8]**	***Pflowr with AC_reac***
1-2	-239.4166	-239.5827	-239.2994
1-4	-172.9834	-172.8173	-173.1006
2-3	6.5317	6.4277	6.5287
2-4	63.0517	62.9895	63.1719
3-4	56.5317	56.4277	56.5287
Avg. Error		0.4080	0.0717

In the next chapter, system partitioning using clustering is discussed along with the application of CF for the IEEE 14 bus test case under base as well as non-base case scenarios.

Chapter 5

SYSTEM PARTITIONING BY BUS CLUSTERING

Clustering techniques are being used for organizing available data into groups. The performance of a clustering algorithm is influenced by spatial relations as well as the distance among the clusters. Mathematically, a cluster is a group of data such that the intra-group distance is smaller than the inter-group distances. In other words, the index of similarity between the buses belonging to a group is greater than that of the members or data of other groups. The larger the deviation between the data sets of different groups as well as larger the similarity between the data sets in the same cluster, the superior the clustering is. At present, there are several types of clustering schemes in theory which have been used to partition a large power system into several small zones. Depending upon the requirement of improving network calculations or performing market analysis, each of the clustering serves a particular purpose. For instance, the techniques described in [13]-[14] deals with expediting certain network computations. In [15]-[18], relevant generators are recognized which are later used for system equivalencing (dynamic). Clustering methods considered in [19]-[20] are ordained for parallel implementation of algorithms regarding power system calculations. The techniques described in [21]-[22] deals with reactive/active power management and market analysis. So, the techniques described in literature works well for their intended purpose, however, they cannot be applied for network reduction based on bus aggregation. So, there is a requirement to look for other clustering schemes which will suit our present objectives. Before proceeding further, the objective of present work is discussed. In context of the present work, clustering is used in order to divide the entire power system network into subsets of buses based on some metric. The partitioning of a larger system plays the most important role in view of defining the topology of the reduced system. The topology of the reduced system comprises of smaller subsets of buses (called as clusters or zones) and inter-zonal links (or aggregated branches) connecting them. The importance of clustering in context of the present requirement can be stated as follows:

(1) It enables us to mathematically determine the organization of zones and the buses present in a zone rather than going for visual partitioning of zones.
(2) Having a mathematical background for partitioning the system results in more accurate inter-zonal power flow between different zones under non-base case operations.

This clustering proves helpful while dealing with a large power system consisting of thousands of buses and transmission lines connecting the buses. Before proceeding further, the basic terms associated with clustering has been discussed. Afterwards, the implementation of two different clustering methods having their own particular benefits have been utilized to partition a power system into smaller zones.

5.1 Basic Terms:

The basic notions in any clustering algorithm is cluster and data. Data can be qualitative (categorical), or quantitative (numerical), or a mixture of both. For the present purpose of partition a power system, only quantitative data (PTDF) is considered. The reason for

considering PTDF as data set is explained in section 5.3.

(a) **Data set**: A data set comprising of ***N*** observations with *n* characteristics is denoted by **Z** = {z_k | k = 1, 2, ... ,N} ,and is represented as an $n \times N$ matrix [23]:

$$Z = \begin{bmatrix} z_{11} & z_{12} & \cdots & z_{1N} \\ z_{21} & z_{22} & \cdots & z_{2N} \\ \vdots & \vdots & \vdots & \vdots \\ z_{n1} & z_{n2} & \cdots & z_{nN} \end{bmatrix} \tag{5.1}$$

Using classical sets, partitions of **Z** can be defined as a family of subsets as:

$$\bigcup_{i=1}^{c} A_i = Z \tag{5.2}$$

The above equation states that A_i includes overall data with *c* being the number of clusters. Mathematically, *Ai* is the union subset. The data set at present will be the PTDF matrix whose columns represent the buses (N) and rows represents the sensitivity factors with respect to different line flows (*n* observations).

(b) **Clusters**: Mathematically, a cluster is a group of data such that the intra-group distance is smaller than the inter-group distances. In other words, the index of similarity between the buses belonging to a group is greater than that of the members or data of other groups. The term coined here called as "similarity" is to be taken in terms of mathematical measurements. In metric spaces, similarity is stated by a *distance norm*. This "distance" has to be calculated between the data vectors and centroids of clusters.

5.2 Types of Clustering

Basically, there are two ways clustering for partitioning a system:

(a) Hierarchical clustering

(b) Partitional clustering

The difference between the above two methods lies in their approach towards breaking down a large system into smaller subsystems. The hierarchical clustering determine successive clusters using previously determined clusters. In hierarchical clustering, the datas or observations are grouped together on the basis of their mutual distances and usually visualized through a hierarchical tree, called as "dendogram tree". This hierarchical tree is a nested set of partitions represented by a tree diagram.

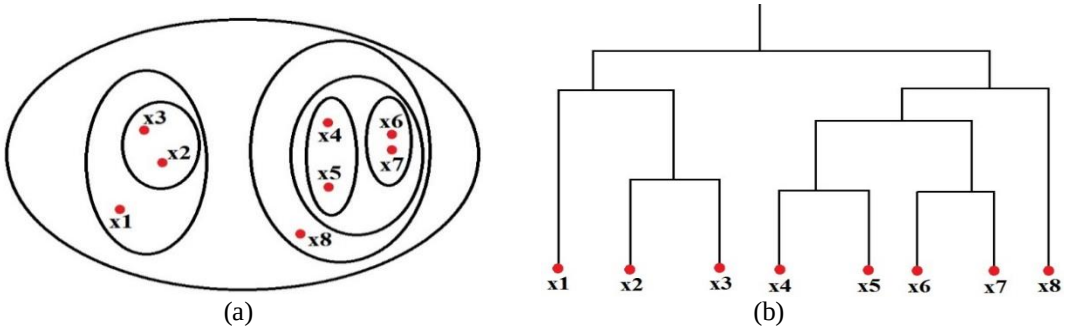

(a) (b)

Fig. 5.1. (a) Hierarchical clustering (b) Dendogram

In contrast to hierarchical clustering, a Partitional clustering divides the actual data set into overlapping or non-overlapping subsets (clusters) such that each observation or data set is present inside only one subset (cluster) or shared by different subsets. In fig.5.2, the entire data set (represented by blue dots) have been separated into three clusters. In the present work, a hard clustering method namely kmeans++ and a soft clustering method namely fuzzy-c-means are used which has been dealt with more elaborately in section **5.5**

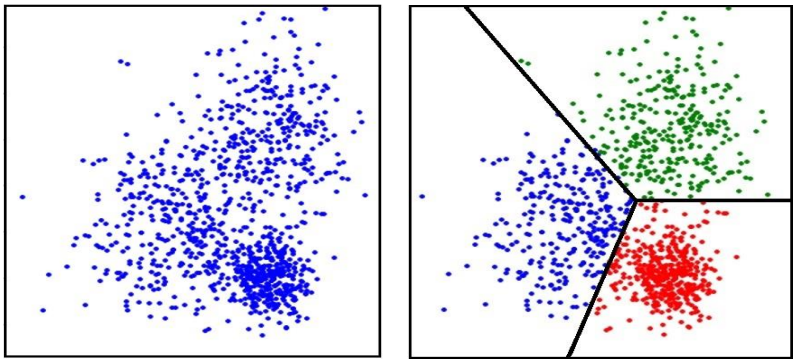

(a) (b)

Fig.5.2. (a) Non-clustered data (b) Clustered data

5.3 Similarity Measure

As mentioned in the beginning of this chapter, the performance of a clustering algorithm is influenced by spatial relations as well as the distance among the clusters. It is the similarity index or metric which determines the data's presence in a particular cluster. Many similarity indices such as the Manhattan distance, the cosine similarity, the Euclidean distance etc. are used. In the clustering techniques to be used here, only the Euclidean distance is used. The Euclidean distance is the length of the straight line which connects two points. For example, let there be two points in Cartesian plane, say x= ($x_1, x_2, x_3, x_4 \ldots x_n$) and y= ($y_1, y_2, y_3, y_4 \ldots y_n$). The Euclidean distance between x and y can be described as:

$$D(x,y) = D(y,x) = \sqrt{(x_1 - y_1)^2 + (x_2 - y_2)^2 + \ldots + (x_n - y_n)^2} \tag{5.3}$$

5.4 Network partitioning by clustering system buses:

It has been stated in previous chapter that, for a small system, system partitioning can be done manually i.e. by prior system knowledge. However, when system partitioning for a large network, say of a large state or even a country's power network, has to be done, then it will be impossible to partition a system by human precision. First of all, one has to understand the reason behind proper partitioning of a large system. The reason for proper partitioning of a system is given below:

In a large power network, large number of buses are present which can have generation sources and loads connected to them. These buses are spread all over the network. Depending upon the location of a particular bus, lines connected to a bus and the line reactances (of the lines connected to a bus) the sensitivity of power flows through different lines get affected. Thus, if buses having somewhat similar sensitivities (to the line power flows) are connected together,

then under non-base case scenarios, the error associated with the inter-zonal power flow can be reduced. In order to perform proper partitioning, clustering algorithms are required. As mentioned previously, kmeans++ and fuzzy-c-means have been used in the present work to partition a large network which in turn is based on minimal Euclidean distance from the cluster centroid [8]. The network partitioning can be done in two cases:

- To study inter-zonal power transactions (market studies): In this case, the PTDF matrix is considered as it is for the dataset to be used in clustering.
- To study power transactions through specific lines required for congestion studies: In this case some of the elements of the PTDF matrix has to be deleted. The procedure can be explained as follows:

  Specific lines are those lines which are operating near their transmission limit and are most likely to get congested in the near future. Determining power flows through such lines will help in taking steps for planning of new lines in the power network or simply to study the effect of adding a distributed generation on the nearly congested lines. In order to preserve the specific lines only in the reduced system, all the rows of the PTDF matrix (except those belonging to the specific lines) have to be deleted prior to clustering. The reduced model so obtained will have the specific lines preserved along with a few number of other inter-zonal lines. For example, let the PTDF matrix be denoted by Φ. After determination of PTDF matrix (Φ), all the rows except belonging to the designated branches are deleted in order to obtain Φ_N as shown in figure below [8]:

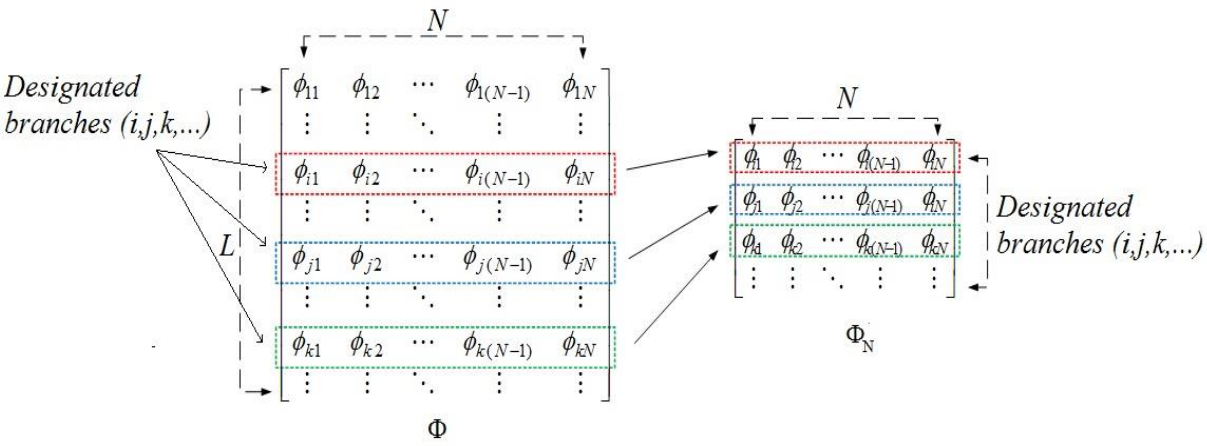

Fig.5.3. Formulation of the PTDF matrix with specific lines only [8]

It should be noted that each column of the PTDF matrix corresponds to the buses in the actual system and hence none of the rows are neither deleted nor changed. After incorporating the above changes, clustering can be applied.

As mentioned previously, two types of clustering schemes (belonging to Partitional clustering) have been used:

(i) kmeans++ clustering

(ii) fuzzy-c-means clustering (fcm)

5.4.1 kmeans++ clustering:

The kmeans++ clustering is same as kmeans clustering but with carefully selected centroids. As mentioned in previous section, the PTDF matrix itself will serve as the data set. In previous chapter, it was mentioned that the number of rows in a PTDF matrix is equal to the number of lines in the actual system and the number of columns in the PTDF matrix is equal to the number of buses (except the slack bus or sink). In terms of mathematical definition, it can be inferred that the network buses (columns of PTDF matrix) are the observations and the lines (rows of the PTDF matrix) are the characteristics. As mentioned earlier, we will proceed with our data set based on our requirement i.e. whether we want to obtain the inter-zonal power flow or we want to obtain power flows through specific lines. If only inter-zonal power flow is our requirement, then we can directly proceed with the PTDF matrix, but if power flow through specific lines is our concern, then we have to take steps as mentioned in the previous page. In both the cases, we have to consider the columns of the PTDF or the new PDTF matrix (with only rows representing the specific lines retained). Let the columns be denoted by CL_i (i=1,2..,N). Thus the PTDF matrix can be considered as an arrangement of columns as PTDF=[CL_1, CL_2,….., CL_N]. Suppose k clusters (partitions of the actual power system) are required. For each of the cluster, a centroid has to be selected which can be done randomly (as in kmeans) or with care (as in kmean++). It has been stated in [24] that the kmeans approach can be utilized for system partitioning into k clusters by making use of Euclidean distance. The presence of CL_i in a cluster depends on the Euclidean distance of CL_i from the cluster's centroid. On applying k-means algorithm, CL_i will belong to a particular cluster such that the Euclidean distance between CL_i and a particular cluster is less than the Euclidean distance between CL_i and any other cluster centroid.

In order to implement kmeans++, the initial centroids have to be selected properly. After proper selection of initial centroid, the basic algorithm as that of kmeans can be used. For initialization of centroids, one has to proceed as follows:

- Step 1: Choose the initial centroid randomly
- Step 2: Compute the Euclidean distance between each CL_i and the prevailing centroids of (say P_1, P_2,….). Let D_{far} be the distance of the farthermost data point from the existing centroids. This farthest data point will be new centroid.
- Step 3: keep on repeating step 2 until the number of centroids is equal to the number of desired clusters.

The process of selection of centroid for kmeans++ is given in fig.5.4.

After the selection of centroid, one can proceed for applying kmeans algorithm [24]. The steps for applying kmeans algorithm are given below:

- Step 1: Calculate the Euclidean distance between different data sets (CL_i) and centroids (P_k). Each data set will be allocated to the centroid having minimum Euclidean distance.
- Step 2: The position of each of the centroids within a cluster are updated by taking the average of all the data sets or vectors present inside the cluster
- Step 3: for the new centroids, check if the conditions stated in step 1 is satisfied, if so, the algorithm converges else repeat step 2.

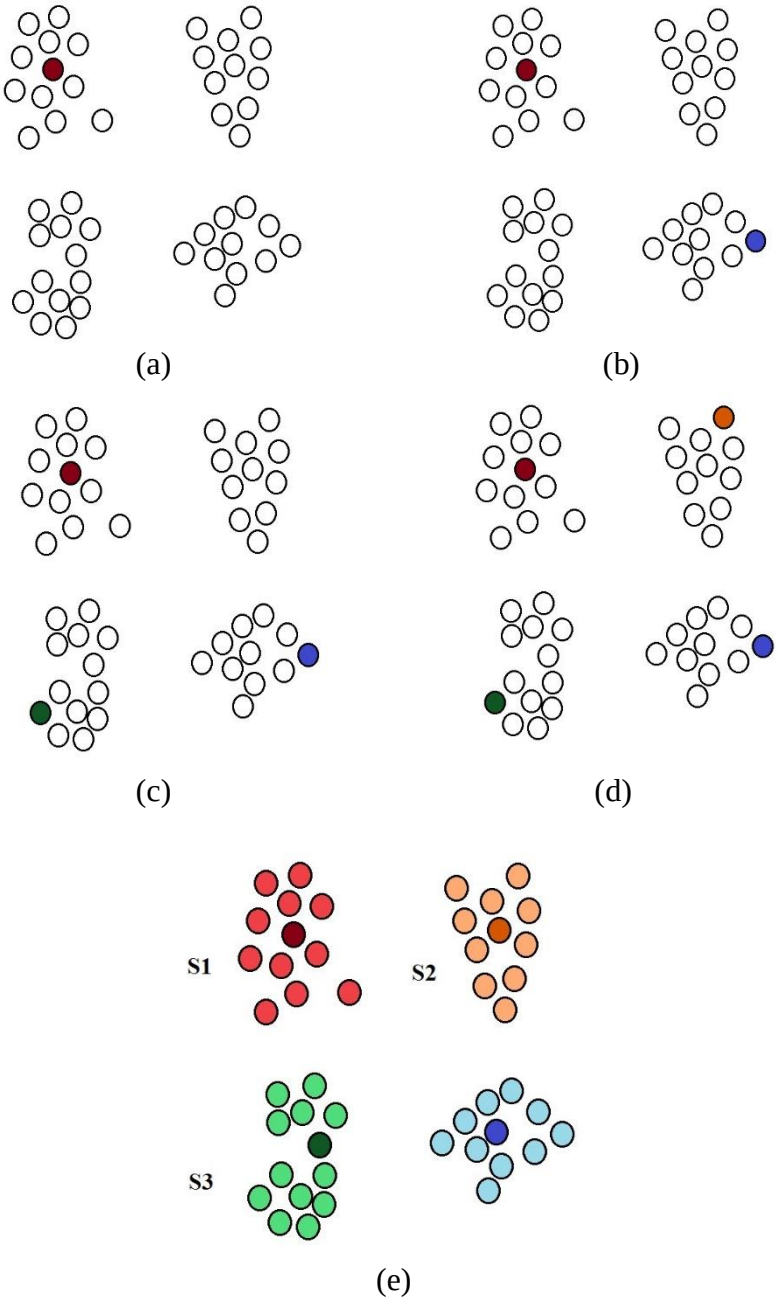

Fig.5.4. Selection of initial centroids is done as in (a),(b),(c),(d). Clustering result is depicted by (e).

The quality of the kmeans or kmeans++ clustering is checked by calculating the Euclidean distance between the centroids to all the data sets present within a cluster. Mathematically, the cluster validity index is called SSE (sum of squared errors) and it is defined as [24]:

$$\mathrm{SSE} = \sum_{a=1}^{k} \sum_{CL \in C_r} dist(D_a, CL)^2 \tag{5.4}$$

where, C_r is the r^{th} cluster

The kmeans++ algorithm has to be applied multiple times (i.e. multiple selection of initial centroids) in order to achieve global minima instead of local minima. The kmeans++ having global minima will yield lowest SSE.

5.4.2 fuzzy-c-means clustering:

The fuzzy-c-means or fcm clustering is a type of soft clustering method in contrast to kmeans++ which is a hard clustering method. The term soft and hard clustering refers to the membership of the data sets within a cluster. In soft clustering method, the membership of a data within a cluster can vary from 0 to 1 (and data finally belonging to cluster having maximum membership value). In hard clustering, a data set has only two membership values: 0 or 1 only. For example, consider that a data set (consisting of 7 elements: $d_1, d_2 \ldots d_7$ i.e. N=7 observations and n=3 characteristics or sensitivities) is partitioned into three clusters, and the partition matrix (U) as obtained by fcm and kmeans++ respectively are as follows:

$$U_{fcm} = \begin{bmatrix} 0.6 & 0.7 & 0.3 & 0.1 & 0.4 & 0.2 & 0.1 \\ 0.1 & 0.1 & 0.3 & 0.5 & 0.1 & 0.7 & 0.1 \\ 0.3 & 0.2 & 0.4 & 0.4 & 0.5 & 0.1 & 0.8 \end{bmatrix}$$

$$U_{kmeans++} = \begin{bmatrix} 1 & 1 & 0 & 0 & 0 & 0 & 0 \\ 0 & 0 & 0 & 1 & 0 & 1 & 0 \\ 0 & 0 & 1 & 0 & 1 & 0 & 1 \end{bmatrix} \tag{5.5}$$

As mentioned before, in fcm, a data set belongs to a cluster having maximum membership. Hence from the above partition matrix it can be seen that each cluster will have similar data's inside them for both kmeans++ and fcm (provided clusters are well separated). From well separated clusters we mean that there will be only a single largest membership value (membership values are the three rows belonging to a particular data/column in U).
So, for a fuzzy partition, the following conditions exists:

$$\mu_{ik} \in [0, 1]; 1 \le i \le c; 1 \le k \le N \tag{5.6a}$$

$$\sum_{i=1}^{c} \mu_{ik} = 1; 1 \le k \le N \tag{5.6b}$$

Also, the fuzzy partitioning space for Z is the set [23]:

$$M_{fc} = \{ U \in \mathbb{R}^{c \times N} \mid \mu_{ik} \in [0,1], \forall i,k; \sum_{i=1}^{c} \mu_{ik} = 1, \forall k; 0 < \sum \mu_{ik} < N, \forall i \} \tag{5.7}$$

Now, fuzzy clustering based on minimization of FCM functional is given by [23]:

$$J(\mathbf{Z};\mathbf{U},\mathbf{V}) = \sum_{i=1}^{c}\sum_{k=1}^{N} (\mu_{ik})^m \| \mathbf{z}_k - \mathbf{v}_i \|_{\mathrm{A}}^2 \tag{5.8a}$$

where,
$$v_i = [\mathbf{v}_1, \mathbf{v}_2, \ldots, \mathbf{v}_c], \quad v_i \in \mathbb{R}^n \tag{5.8b}$$

and
$$D_{ik\mathbf{A}}^2 = \| \mathbf{z}_k - \mathbf{v}_i \|_{\mathrm{A}}^2 = (\mathbf{z}_k - \mathbf{v}_i)^T \mathrm{A} (\mathbf{z}_k - \mathbf{v}_i) \tag{5.8c}$$

V is a vector of cluster prototypes (centers) which have to be determined and $D_{ik\mathbf{A}}^2$ is a squared inner-product distance norm or Euclidian norm. Also:

$$m \in [1, \infty) \tag{5.9}$$

where, m is a parameter called fuzzy partition matrix exponent (FPME) which determines fuzziness of the resulting clusters [23],[25].

By applying Picard iteration to the objective function J in (5.8a), the stationary points of J can be determined by adjoining the constraint of (5.6b) to J by means of Lagrange multipliers and by setting the gradients of $\bar{J}$ with respect to $\mathbf{U}, \mathbf{V}$ and λ to zero:

$$\bar{J}(\mathbf{Z};\mathbf{U},\mathbf{V},\lambda) = \sum_{i=1}^{c}\sum_{k=1}^{N}\left(\mu_{ik}\right)^{m} D_{\mathrm{ikA}}^{2} + \sum_{k=1}^{N}\lambda_{k}\left[\left(\sum_{i=1}^{c}\mu_{ik}\right)-1\right] \tag{5.10}$$

Also, if $D_{ik\mathbf{A}}^{2} > 0, \forall\, i,k$ and m >1, then (U,V) will minimize only if :

$$\mu_{ik} = \frac{1}{\sum_{j=1}^{c}\left(\frac{D_{ik\mathbf{A}}}{D_{jk\mathbf{A}}}\right)^{\frac{2}{m-1}}}; \quad 1 \le k \le \mathrm{N},\ 1 \le i \le \mathrm{c} \tag{5.11}$$

and

$$v_i = \frac{\sum_{k=1}^{N}\left(\mu_{ik}\right)^{m}\mathbf{z}_k}{\sum_{k=1}^{N}\left(\mu_{ik}\right)^{m}}; \quad 1 \le i \le \mathrm{c} \tag{5.12}$$

With the above-mentioned background, one can apply the fuzzy c-means technique in order to partition the system. Here again, the PDTF matrix will be our data set matrix **Z** (for congestion profile, follow the steps mentioned in [8] to obtain the new PTDF matrix which will comprise of only the congested lines). In this work, the application of fcm is stressed because the quality of clustering performed by kmeans++ solely depends upon SSE. By dealing with certain test cases, it has been found that network partitioned through kmeans++ has low SSE, but it may not be practically feasible. Moreover, an individual cannot control the way kmeans++ work (except selecting the initial centroid). Although, after clustering, we can manually shift a data-set from one cluster to another and proceed (but it will be very difficult for a very large network), but it will be more viable if the clustering itself can be controlled and proper partitioning is performed. For these reasons, a soft clustering technique called the fcm is applied. The fcm can be controlled by selection of FPME (*m*) mentioned in eqn.(5.9). As *m* tends to unity value, the clustering become more crisp, and as *m* tends to positive infinite, clustering becomes more and more fuzzy (in the fizziest partition, all the dataset will belong to only one cluster). It should be kept in mind that partitions provided by kmeans++ and by fcm with high crispness ($m \approx 1$) are different.

As one can check the quality of clustering of kmeans++ by SSE, one can check the quality of clustering performed by fcm through Xie-Beni index. Xie and Beni defined the total variation σ of (U,V) and the separation $sep(V)$ of the vectors V as [26]:

$$\sigma(\mathrm{Z}\,;\,\mathrm{U},\mathrm{V}) = \sum_{i=1}^{k}\left(\sum_{y=1}^{N}\mu_{iy}^{m}\ \|\, z_y - v_i \,\|^{2}\right) \tag{5.13}$$

$$sep\ (\mathrm{V}) = \min_{\mathrm{i,y}}\left(\|\, v_i - v_y \,\|^{2}\right) \tag{5.14}$$

One can see that eqn.(5.13) can yield SSE (in case of kmeans++) if μ_{ik} is only 0 or 1.

Based on the above two terms, Xie and Beni formulated the Xie-Beni index as [26]:

$$\mathrm{XB} = \frac{\left(\frac{\sigma}{N}\right)}{sep\ (\mathrm{V})} \tag{5.15}$$

or,

$$\mathrm{XB} = \frac{\sum_{i=1}^{k}\sum_{k=1}^{N}\mu_{iy}^{m}\ \|z_y - v_i\|^2}{N\ (\min_{i,y}\|v_i - v_y\|^2)} \tag{5.16}$$

It was mentioned in [26] that a good (U,V) pair will yield a small value of σ because μ_{ik} is expected to be high when $\|z_k - v_i\|$ is low. Alongside, well separated v_i's will give a high value of *sep*(V)(i.e. greater inter-cluster separation). By reducing *m* (which will in turn increase the membership values of data sets in clusters) the numerator of (22) can be affected and thus help us in achieving a system partition with lower XB index. In [27] it was stated that clusters quality has been determined with different values of *m* whereas for determining optimal number of clusters, *m* was suggested to be in the range [1.5, 2.5]. [28] determined the optimal value of *m* to be [1.25,1.75]. In terms of algorithm convergence, [29] proposed that *m* should be greater than $[N/(N-2)]$. So, from previously available literature, it should be understood that variation of *m* depends upon the application of fcm. At present, by varying *m* and applying it to different scenarios (various small and large test cases), it was found out that our purpose will be fulfilled by varying *m* between 1.1 to 1.5. Below 1.07 there were convergence issues for very large systems and so to be on the safer side, values greater than 1.1 are recommended. Above 1.5, clusters will not be well separated (in terms of fcm partitioning) which can be observed from lower membership values in U. Following observations has been made after going through several small, medium and large network partitioning:

(a) if $1.4 < m < 1.5$, clusters same as kmeans++ is obtained.
(b) if $1.1 < m < 1.4$, clusters are obtained with lower XB as compared to kmeans++ (values near to 1.1 and near to 1.4 are preferable for larger and smaller systems respectively).

The objective behind controlling *m* is to improve the membership values in U (which is the indication for relocating centroids so that intra-cluster separation is low). Intra-cluster separation is low with higher membership values (and thus lower value of *m*). It should be noted that the intra-cluster separation in kmeans++ only relies on Euclidian distance whereas the intra-cluster separation in fcm relies on Euclidian distance as well as on *m* and μ. It has been observed that those partitions obtained by kmeans++ are relatively more fuzzy (i.e. data have lower membership values) when the same partitions (as obtained by kmeans++) are obtained by fcm. More crispness is induced in fcm by improving the membership values (which in turn is achieved by lowering the value of *m*). By crispness here, we mean that the membership values are higher in a particular cluster as compared to membership values in other clusters. The crispier the partitions are (in terms of fcm), the lower will be numerator in (22) which will result in low XB index. The results of different clustering on IEEE 14 bus system is discussed in section 5.5.

The fuzzy c-means algorithm (FCM) applied here is stated below [23]:

Step 1: Select PTDF matrix as the data set **Z**

Step 2: set the number of clusters $1<k<N$, the termination tolerance $\varepsilon > 0$ (here $\varepsilon = 0.001$) and the weighting exponent $1.1<m<1.4$.

Step 3: initialize the partition matrix randomly.

Step 4: compute the cluster prototypes (means/ centroids):

$$v_i^{(l)} = \frac{\sum_{y=1}^{N} \left(\mu_{iy}^{(l-1)}\right)^m \mathbf{z}_y}{\sum_{y=1}^{N} \left(\mu_{iy}^{(l-1)}\right)^m}; \quad 1 \le i \le \mathrm{c}$$

Repeat for *l* = 1, 2…

Step 6: Calculate the distances:

$$D_{ik\mathbf{A}}^2 = (\mathbf{z}_k - \mathbf{v}_i^{(l)})^T \mathrm{A} (\mathbf{z}_k - \mathbf{v}_i^{(l)})$$

Step 7: Update the partition matrix:

If $D_{ik\mathbf{A}} > 0$ for i=1,2…..c; then:

$$\mu_{ik}^{(l)} = \frac{1}{\sum_{j=1}^{k} \left(\frac{D_{iy\mathbf{A}}}{D_{jy\mathbf{A}}}\right)^{\frac{2}{m-1}}}; \quad 1 \le y \le \mathrm{N},\ 1 \le i \le k$$

until $\left\|\bar{U}^{(l)} - \bar{U}^{(l-1)}\right\| < \varepsilon$.

Otherwise (if $D_{ik\mathbf{A}} = 0$):

$$\mu_{ik}^{(l)} = 0, \text{ and } \mu_{ik}^{(l)} \in [0,1] \text{ with } \sum_{i=1}^{c} \mu_{ik}^{(l)} = 1$$

From step 4, the cluster centroids dependency on m and μ can be seen.

5.5 Results

In order to visualize the importance of applying fcm over kmeans++, both the clustering techniques have been applied on the IEEE 14 bus test case.

The partitioned systems are shown in fig.5.5.

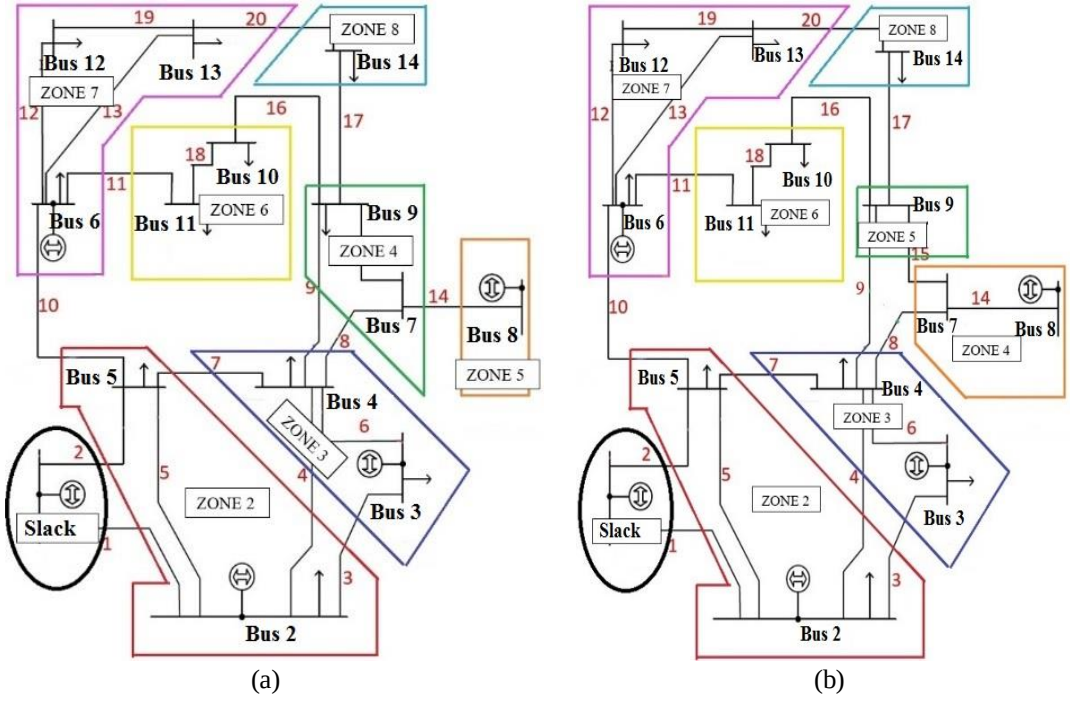

Fig.5.5. IEEE 14 bus system partitioned into 8 zones by (a) kmeans++ clustering (also with fcm by taking m = 1.4) (b) fuzzy-C-means clustering (by taking m = 1.3).

The sensitivities (PTDF's) of the lines with respect to bus 7,bus 8 and bus 9 are given in Table 5.1.

Table 5.1. Sensitivities Of Bus 7, Bus 8 and Bus 9

Lines	Bus 7	Bus 8	Bus 9
1	-0.6573	-0.6573	-0.6519
2	-0.3427	-0.3427	-0.3481
3	-0.1427	-0.1427	-0.1382
4	-0.2987	-0.2987	-0.2891
5	-0.2159	-0.2159	-0.2246
6	-0.1427	-0.1427	-0.1382
7	0.3589	0.3589	0.2830
8	-0.6342	-0.6342	-0.4513
9	-0.1661	-0.1661	-0.2590
10	-0.1997	-0.1997	-0.2897
11	-0.1202	-0.1202	-0.1744
12	-0.0177	-0.0177	-0.0256
13	-0.0618	-0.0618	-0.0896
14	0.0000	-1.0000	0.0000
15	0.3658	0.3658	-0.4513
16	0.1202	0.1202	0.1744
17	0.0794	0.0794	0.1152
18	0.1202	0.1202	0.1744
19	-0.0177	-0.0177	-0.0256
20	-0.0794	-0.0794	-0.1152

The kmeans++ includes buses 7 and 9 in a single zone whereas fcm includes buses 7 and 8 in a single zone.One can see that all the elements of bus 7 and 8 are same except at the 14^{th} line, the reason being bus 8 is connected radially to bus 7. Now, mathematically speaking, the overall spatial distance between bus 7 and bus 8 is slightly more than that of bus 7 and bus 9 and so kmeans++ puts bus 7 and bus 9 together and bus 8 separately. But owing to the sensitivity of the buses,it will be more practical to accommodate bus 7 and bus 8 in a single zone as shown in fig.5(b). When fcm was applied on the 14 bus system, partitions were obtained as:

- Same as fig.5.5 (a) i.e. same as kmeans++ with m = 1.4. The highest values of membership value in each cluster varied from 0.89 to 0.93. Also, XB = **2.8722**
- As in fig.5.5 (b) with m = 1.3. The highest values of membership value in each cluster varied from 0.96 to 1. Also, XB = **2.6216**

Hence, it can be seen that XB is a better cluster validity index as compared to SSE for practical purposes. The reduced model of fig.5(b) will be used in section IV for carrying out

load flow analysis. For calculating inter-zonal power flow, the system in fig.5.5(b) is considered (which is obtained through fcm). The reduced model of fig.5.5(b) is shown in fig.5.6.

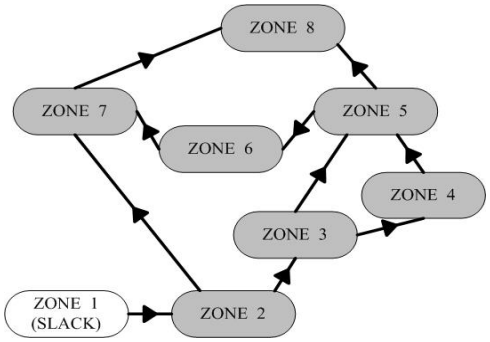

Fig.5.6. Equivalent 8 zone model of IEEE 14 bus test case

As mentioned in the previous chapter, the Correction Factor(CF) is also used for improving the accuracy of the inter-zonal power flows. Likewise previous chapter, CF is calculated as:

$$[CF] = \frac{[P_{\text{flow}}^{\text{inter-zonal}}]\big|_{NR}}{[PTDF_R] \times [(P_{\text{inj}})_R]} \tag{5.17}$$

The DC_reac, CF and AC_reac for the 8 zone system is shown in Table 5.2.

Table 5.2. Line reactances and correction factor

***DC_reac* [8]**	***Correction Factor***	***AC_reac***
0.1619	1.0000	0.1619
0.0008	0.9944	0.0008
0.2128	1.0248	0.2076
0.1824	0.9781	0.1865
0.4826	0.9753	0.4948
0.0945	0.9781	0.0966
0.1944	0.9067	0.2144
0.202	0.9530	0.212
0.0663	1.0917	0.0607
0.2446	1.0937	0.2236

In order to check the robustness of the reduced system, load flow of IEEE 14 bus system is carried out for:

- Base-case.
- Non-base case i.e. the net injected power at the buses is changed between -10% to +10%

The load flow results for the above two cases are shown in Table 5.3 and Table 5.4.

Table 5.3. Power Flows at base case

Inter-links	***Pflow by NR in the original system***	***Pflowr with DC_reac* [8]**	***Error %***	***Pflowr with AC_reac***	***Error %***
I-II	219.0000	219.0000	0	219.0000	0
II-III	186.5717	187.6079	-0.5554	186.5609	0.0058
II-VII	43.1283	42.0921	2.4026	43.1391	-0.0250
III-IV	28.3515	28.9801	-2.2172	28.3439	0.0268
III-V	16.2202	16.6278	-2.5129	16.2170	0.0197
IV-V	28.3515	28.9801	-2.2172	28.3439	0.0268
V-VI	5.6170	6.1897	-10.1958	5.6108	0.1104
V-VIII	9.4547	9.9182	-4.9023	9.4501	0.0487
VI-VII	-6.8830	-6.3103	8.3205	-6.8892	-0.0901
VII-VIII	5.4453	4.9818	8.5119	5.4499	-0.0845
Mean error %			4.1836		0.0438

Table 5.4. Power Flows at non-base case

Inter-links	***Pflow by NR in the original system***	***Pflowr with DC_reac* [8]**	***Error %***	***Pflowr with AC_reac***	***Error %***
I-II	223.258	223.258	0	223.258	0
II-III	190.087	191.153	-0.5608	190.082	0.0026
II-VII	43.842	42.776	2.4315	43.847	-0.0114
III-IV	28.755	29.402	-2.2500	28.750	0.0174
III-V	16.449	16.869	-2.5533	16.449	0
IV-V	28.755	29.402	-2.2500	28.750	0.0174
V-VI	5.821	6.386	-9.7062	5.800	0.3608
V-VIII	9.884	10.385	-5.0688	9.899	-0.1518
VI-VII	-7.053	-6.489	7.9966	-7.074	-0.2977
VII-VIII	5.760	5.259	8.6979	5.745	0.2604
Mean error %			4.151		0.112

The fcm clustering along with the correction factor (CF) has also been applied to actual Indian Power System (at transmission level) and it has been presented in the next chapter.

Chapter 6

REDUCED EQUIVALENT OF INDIAN POWER SYSTEM

In this chapter, a reduced equivalent model of the actual Indian Power system is presented. The actual Indian Power system which consists of 6034 buses and 8116 lines have been reduced to an equivalent network consisting of 120 buses and 216 lines. The improvement in accuracy as compared to prior methods [8] is shown with respect to the load flow result obtained through conventional Newton Raphson's method.
In the text to be followed, a brief review of the actual Indian power system is given followed by an equivalent reduced network in order to determine the inter-zonal power flow.

6.1 Indian Power System:

The Indian Power System considered here corresponds to the "All India Peak" as on "August 2013". With over 280,000 circuit kilometers, India's transmission network is one of the largest network in the world. Previously, the whole network was divided in five regions consisting of buses at various voltage levels as [30]:

- 765kV : 7910 ckm
- 400kV : 1,20,693 ckm
- 220kV : 1,42,536 ckm
- HVDC Bipole (±500kV) : 9,432 ckms

At present, all the five regions are synchronously connected. It consists of 6034 buses (generators are connected to 575 buses and loads are connected to 3422 buses) connected by 8116 lines: were reported operational at the summer peak of August 2013. The net generation is 120.213 GW whereas the load is 117.809 GW (the losses being 2.403GW i.e. 1.998% of the total generation). A snapshot of the Indian power system [32] is shown in fig.6.1.

6.2 Reduced Equivalent Network:

As mentioned above, a reduced equivalent comprising of 120 zones interconnected by 216 lines is presented in Fig.6.1 and the same reduced network based on the location of the zones on the Indian map is shown in Fig.6.2. On account of using the correction factors in fine tuning the reactances, the accuracy of the inter-zonal power flow has been improved significantly and a comparison of the same has been presented in Table 6.1. From Table 6.1, it can be observed that: out of 216 lines (power flows), the power flow at 212 lines have been improved using AC_reac. The four lines where DC_reac provides better power flow are: 61, 116, 201 and 207. It can be seen from Table 6.1 that for a large system, though the mean absolute error using DC_reac is not large, but the error associated with individual lines can be large. The presence of zero flow error at various lines is due to some of the zones being radially connected to the larger mesh network.

Therefore, it is encouraged to make use of the correction factor for fine tuning the line reactances in the reduced system on account of improved accuracy in comparison to the result obtained through empirical methods (conventional Newton Raphson load flow).

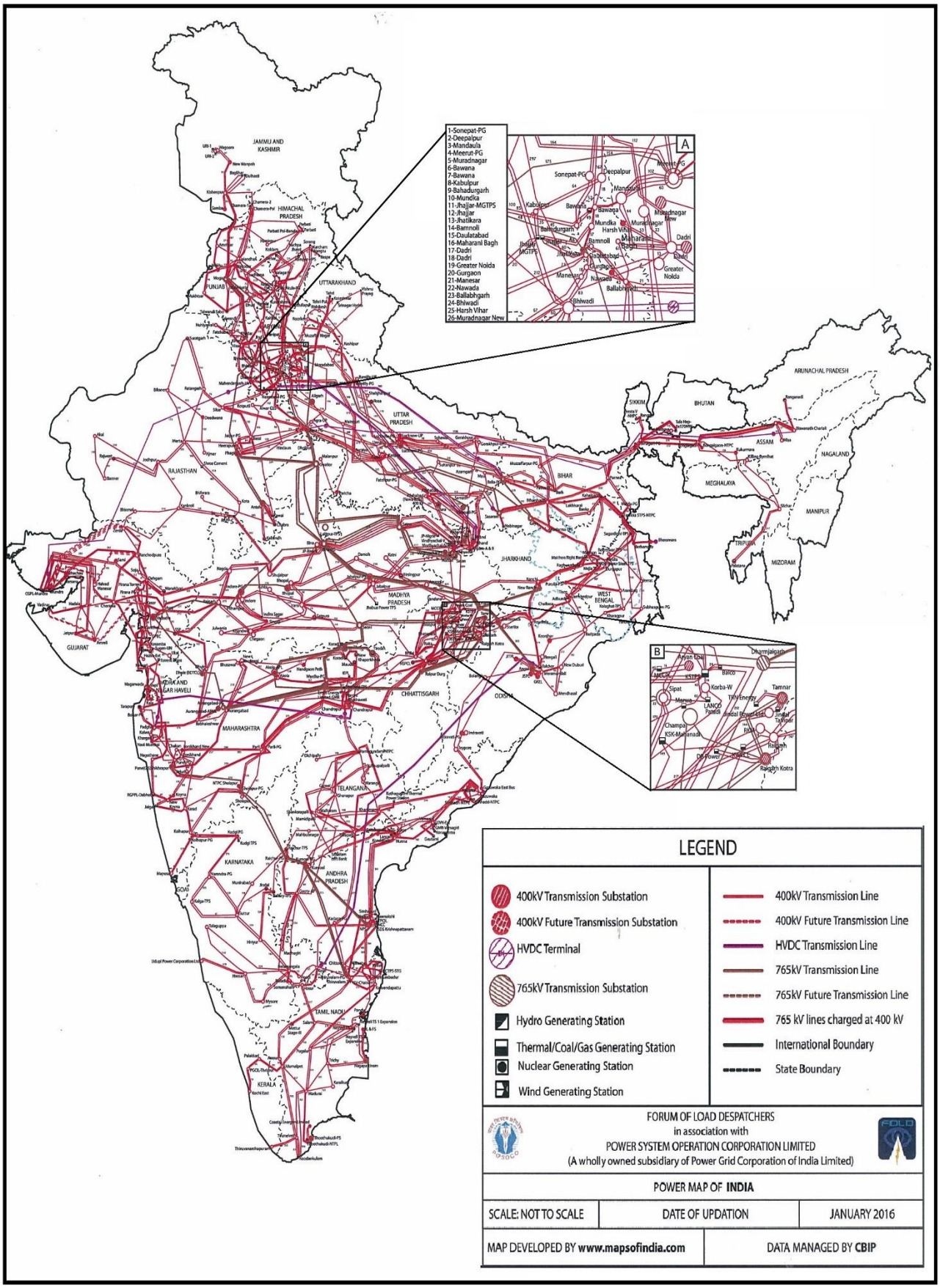

Fig. 6.1 Indian Power System

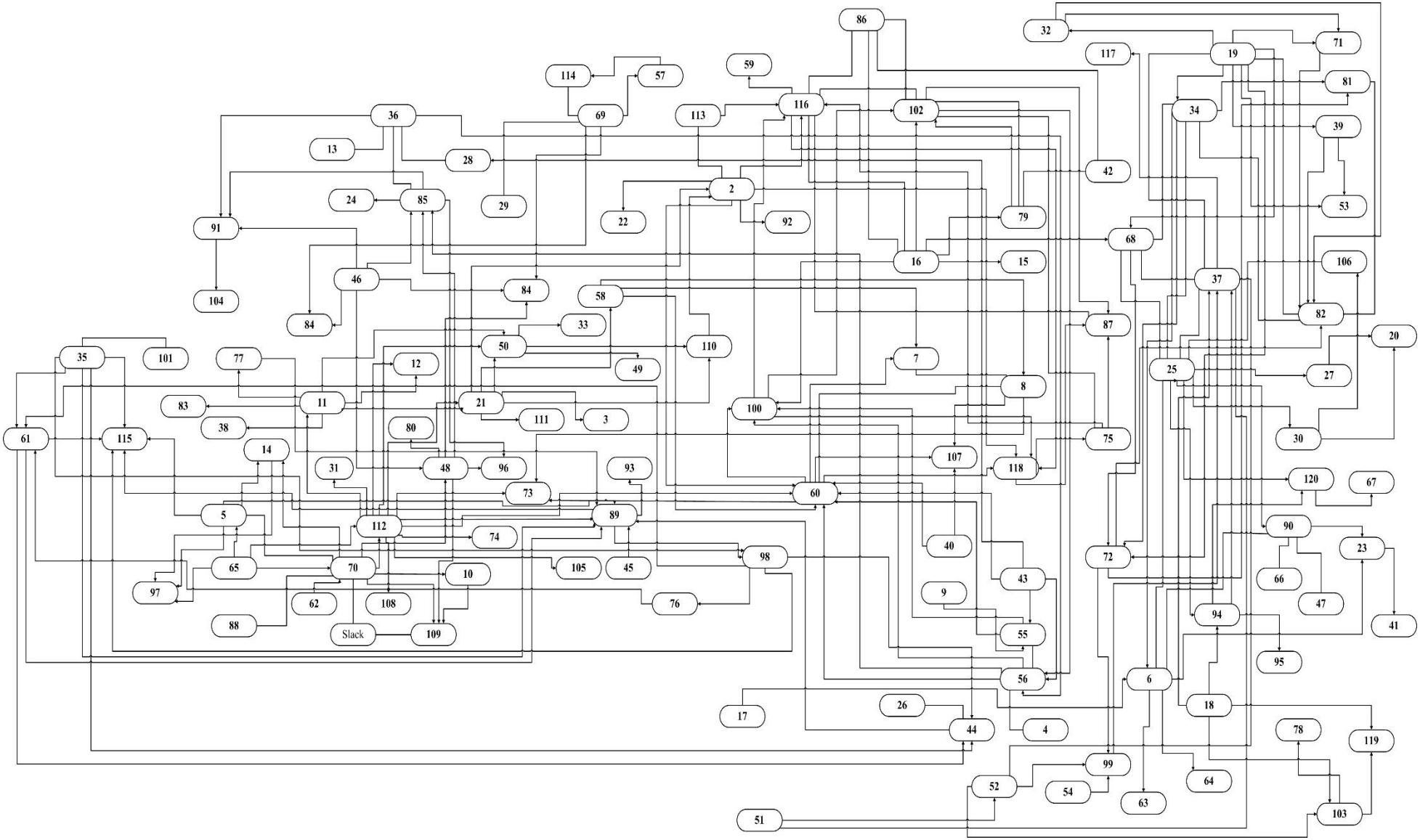

Fig. 6.2 Reduced equivalent comprising of 120 zones and 216 lines

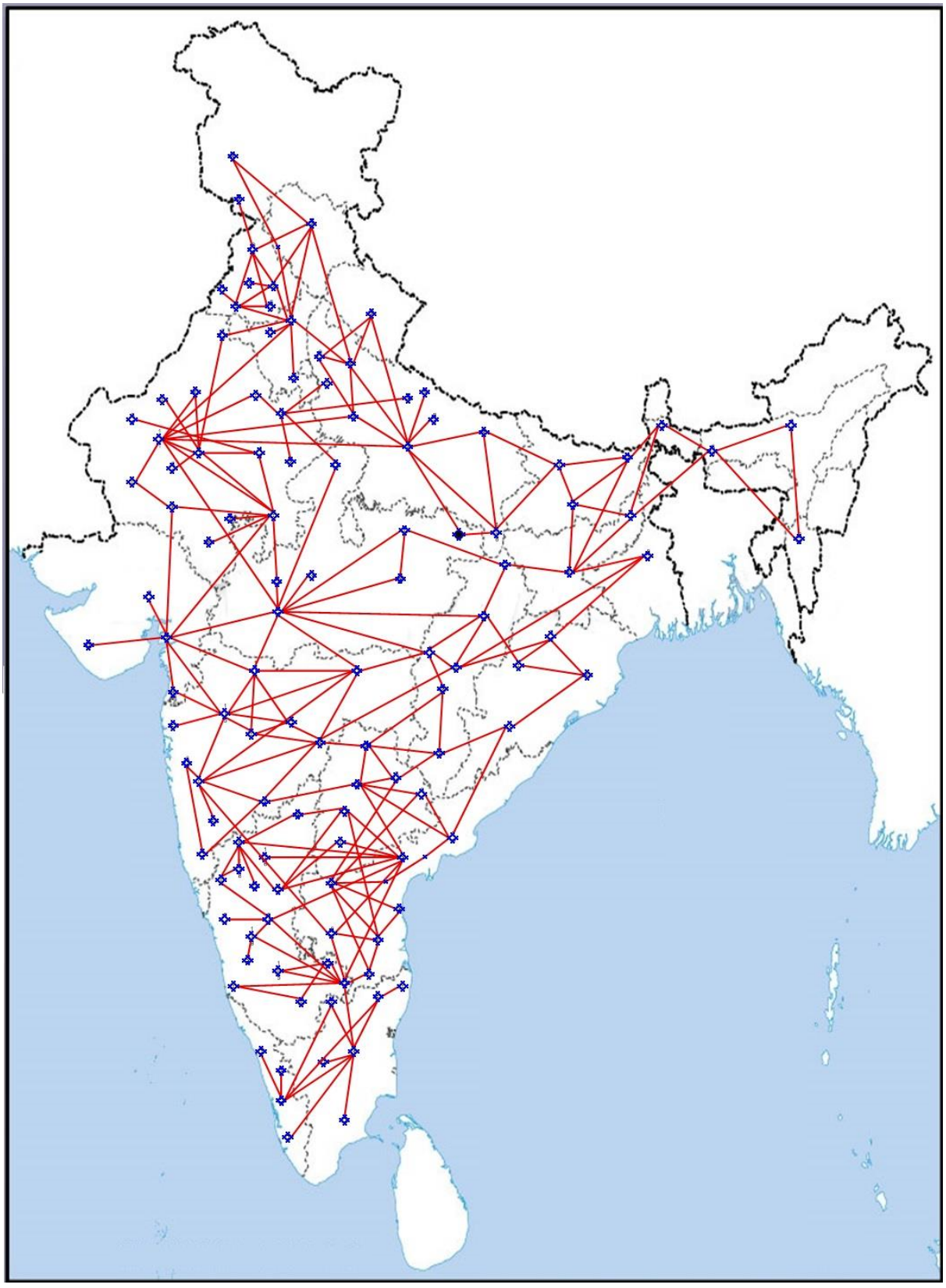

Fig. 6.3 Reduced Indian Power System on Indian Map

Table 6.1 Comparison of Power Flows at base case

Lines	Actual Power flow obtained by *NR*	*PTDFr*Pr* [8] 'or' Power flow with *DC_reac*	Error *%*	Power flow with *AC_reac*	Error *%*
1-70	-1472.76	-1449	1.612958	-1472.71	0.003306
1-109	-930.546	-954.301	-2.55279	-930.595	-0.00523
2-21	176.6963	192.9733	-9.21186	176.7485	-0.02955
2-22	-3644.61	-3644.61	0	-3644.61	0
2-60	-1186.29	-1124.72	5.190461	-1186.51	-0.01801
2-92	135.586	135.586	0	135.586	0
2-110	196.7128	209.3983	-6.44873	196.7093	0.001779
2-113	1424.115	1405.801	1.285996	1424.089	0.001862
2-116	377.2026	310.071	17.79722	377.3837	-0.04801
2-118	7.845219	2.75438	64.89097	7.855613	-0.13249
3-21	-325.044	-325.044	0	-325.044	0
4-56	1536.071	1536.071	0	1536.071	0
5-14	351.3967	343.7471	2.176919	351.3849	0.003351
5-65	-217.712	-218.937	-0.5626	-217.662	0.023246
5-70	-1458.86	-1447.66	0.767572	-1458.93	-0.00497
5-89	-10.6518	-2.90722	72.7069	-10.6476	0.039285
5-97	128.8725	121.1349	6.004078	128.8682	0.003357
5-115	-52.529	-54.8593	-4.43629	-52.4952	0.064379
6-17	290.64	290.64	0	290.64	0
6-23	373.6191	370.4987	0.835185	373.6162	0.000779
6-25	-154.777	-153.271	0.973501	-154.787	-0.00652
6-34	-53.1282	-50.7467	4.482561	-53.1131	0.028525
6-63	187.844	187.844	0	187.844	0
6-64	-587.643	-587.643	0	-587.643	0
6-90	652.7405	651.9726	0.117635	652.7383	0.000331
7-8	-34.8182	-33.9332	2.541761	-34.8235	-0.0155
7-58	368.4704	374.4209	-1.61492	368.3373	0.036125
7-60	-879.574	-886.41	-0.77714	-879.436	0.015747
8-58	12.21461	12.98778	-6.32987	12.21779	-0.02606
8-60	-440.239	-462.978	-5.16521	-440.235	0.000865
8-73	338.5442	344.1144	-1.64534	338.5191	0.007389
8-107	-680.96	-663.679	2.537724	-680.948	0.001854
9-55	-35.926	-35.926	0	-35.926	0
10-70	-295.872	-286.081	3.30919	-295.884	-0.004
10-109	-567.28	-577.071	-1.72595	-567.268	0.002088
11-12	185.367	187.4744	-1.13687	185.367	-1.08E-07
11-21	26.84804	24.94602	7.084398	26.84478	0.012134
11-38	204.887	204.887	0	204.887	0
11-50	29.84613	25.72473	13.80884	29.81987	0.087989
11-77	323.4269	324.3755	-0.29329	323.4266	0.00011
11-83	73.089	73.089	0	73.089	0
11-112	-119.09	-116.123	2.491767	-119.06	0.025085
12-112	-187.014	-184.907	1.126862	-187.014	1.07E-07
13-36	-254.692	-254.692	0	-254.692	0

14-70	-549.438	-552.554	-0.56722	-549.453	-0.00274
14-97	75.56456	71.03146	5.99897	75.56785	-0.00437
15-16	-390.964	-390.964	0	-390.964	0
16-68	2379.002	2379.002	0	2379.002	0
16-79	-51.317	-59.4166	-15.7836	-51.3164	0.001087
16-86	-769.663	-740.625	3.772895	-769.634	0.00376
16-100	-2099.92	-2158.12	-2.77168	-2099.95	-0.00152
16-102	-332.626	-333.252	-0.18808	-332.624	0.000807
16-116	58.54443	96.43409	-64.7195	58.54422	0.000351
18-37	-7.7565	-7.80709	-0.65227	-7.75626	0.003101
18-94	-347.388	-347.091	0.085529	-347.397	-0.00248
18-103	163.8696	163.6637	0.125642	163.878	-0.0051
18-119	0.111058	0.070424	36.58775	0.111063	-0.00512
19-32	-102.366	-104.98	-2.55345	-102.336	0.029147
19-34	324.3052	320.4867	1.177438	323.8228	0.148759
19-37	-459.122	-456.166	0.643925	-459.294	-0.03736
19-39	-42.5973	-43.9359	-3.14249	-40.4402	5.063896
19-53	994.4943	994.5809	-0.00871	994.5686	-0.00747
19-68	-117.74	-117.586	0.130147	-117.74	-8.19E-05
19-71	-305.082	-306.917	-0.60168	-304.984	0.032112
19-72	321.5227	326.5456	-1.56222	321.0628	0.143058
19-82	-585.955	-584.568	0.23678	-587.2	-0.2125
20-27	-158.033	-156.388	1.040623	-158.032	0.000493
20-30	9.323882	7.679356	17.63778	9.323104	0.008351
21-50	197.6628	207.1075	-4.77818	197.6389	0.012094
21-58	-167.826	-173.474	-3.3655	-167.633	0.114526
21-110	115.345	106.4637	7.699744	115.3419	0.002705
21-111	198.906	198.906	0	198.906	0
21-112	958.1112	977.5709	-2.03105	957.9949	0.012131
23-41	71.156	71.156	0	71.156	0
23-90	155.4041	152.2837	2.007934	155.4012	0.001874
24-85	-303.478	-303.478	0	-303.478	0
25-27	287.5189	285.8744	0.571972	287.5181	0.000271
25-30	76.58763	77.58595	-1.3035	76.5881	-0.00062
25-34	54.00272	71.5918	-32.5707	54.00735	-0.00857
25-37	-554.473	-557.696	-0.58123	-554.36	0.020352
25-68	-913.992	-932.385	-2.01239	-914.125	-0.01449
25-90	117.9864	121.8747	-3.29552	117.9915	-0.0043
25-94	-705.806	-705.206	0.085028	-705.806	-2.48E-05
25-106	52.51349	53.1597	-1.23056	52.51379	-0.00058
25-120	-23.6775	-22.6324	4.414241	-23.6776	-0.00015
26-44	-267.725	-267.725	0	-267.725	0
28-36	-175.882	-177.061	-0.6702	-175.836	0.026587
28-43	209.9475	211.1262	-0.56145	209.9007	0.022273
29-69	161.891	161.891	0	161.891	0
30-106	5.141509	4.495301	12.56845	5.141206	0.005895
31-112	-260.314	-260.314	0	-260.314	0
32-71	-108.213	-109.511	-1.19971	-108.248	-0.03239
32-82	694.2714	692.9558	0.189497	694.3363	-0.00935
33-50	-93.446	-93.446	0	-93.446	0
34-68	-1172.17	-1157.46	1.254971	-1171.99	0.015625
34-72	-130.737	-134.861	-3.15432	-130.528	0.15974
34-81	-10.0994	-12.4513	-23.2871	-10.1181	-0.18438

34-82	-495.234	-487.317	1.598716	-496.07	-0.16881
35-44	63.46477	64.5974	-1.78466	63.468	-0.00508
35-61	124.2138	124.9272	-0.57431	124.2329	-0.01535
35-89	358.1765	365.5656	-2.06295	358.9153	-0.20625
35-98	-96.6095	-103.263	-6.88733	-97.2141	-0.62585
35-101	220.356	220.356	0	220.356	0
35-115	-99.9257	-102.507	-2.58312	-100.082	-0.15654
36-56	-340.468	-333.05	2.178979	-340.822	-0.10372
36-85	1412.31	1386.977	1.793718	1412.621	-0.02205
36-91	709.9263	726.6616	-2.35734	710.0147	-0.01246
37-51	86.54552	86.5864	-0.04723	86.54616	-0.00074
37-52	82.74466	82.50987	0.283751	82.74432	0.000402
37-68	-365.761	-363.819	0.531088	-365.844	-0.02265
37-94	13.62562	11.68319	14.25572	13.63444	-0.06472
37-99	211.3009	210.3689	0.441055	211.3178	-0.00801
37-103	63.41467	64.22349	-1.27544	63.41303	0.002587
37-117	116.244	116.244	0	116.244	0
39-53	-28.9653	-29.0519	-0.29903	-29.0396	-0.25645
39-82	-283.776	-285.028	-0.44119	-281.545	0.786312
40-60	-204.464	-206.67	-1.07892	-204.462	0.001039
40-107	-94.206	-92	2.341673	-94.2081	-0.00225
42-79	12.77991	9.491265	25.73296	12.77974	0.001339
42-86	-171.405	-168.116	1.918644	-171.405	9.98E-05
43-55	286.7762	289.0273	-0.78496	286.8422	-0.02302
43-56	-172.236	-174.076	-1.06837	-172.372	-0.07896
43-60	100.9615	101.7293	-0.76048	100.9847	-0.02302
44-61	242.5717	235.8861	2.756145	242.6113	-0.01635
44-89	-715.904	-706.276	1.344784	-715.94	-0.00513
44-98	-15.5232	-17.3323	-11.6541	-15.523	0.001673
45-89	-445.629	-445.629	0	-445.629	0
46-48	550.3137	556.465	-1.11778	550.4299	-0.02113
46-84	-172.58	-176.45	-2.24235	-172.581	-0.00076
46-85	-647.932	-648.477	-0.08411	-648.042	-0.01702
46-91	-17.963	-19.6995	-9.66693	-17.9677	-0.0261
47-90	-268.243	-268.243	0	-268.243	0
48-70	3210.112	3162.461	1.484401	3210.555	-0.01381
48-80	406.283	406.283	0	406.283	0
48-84	-1278.76	-1274.89	0.302625	-1278.76	0.000103
48-85	-2721.42	-2704.11	0.636022	-2721.87	-0.01634
48-96	129.6763	129.3809	0.227773	129.6696	0.005145
48-109	943.3157	976.2346	-3.4897	943.4386	-0.01303
49-50	68.148	68.148	0	68.148	0
50-110	78.82018	75.01597	4.826441	78.8268	-0.0084
50-112	141.6938	150.8212	-6.44171	141.637	0.040076
51-52	32.25552	32.2964	-0.12672	32.25616	-0.00199
52-99	-36.6855	-36.3171	1.004162	-36.6784	0.01918
52-103	43.20864	42.64635	1.301351	43.20191	0.015572
54-99	-36.898	-36.898	0	-36.898	0
55-56	-724.339	-691.973	4.468318	-724.268	0.009749
55-60	-344.802	-377.412	-9.45773	-342.742	0.597477
55-100	397.948	400.4437	-0.62716	395.8833	0.518843
56-60	2176.941	2099.746	3.546056	2176.729	0.009756
56-85	242.7813	236.6468	2.526763	242.9478	-0.06857

56-100	2445.024	2569.241	-5.08041	2444.786	0.009741
56-102	845.1631	842.2204	0.34818	845.0287	0.015908
57-69	-361.745	-361.999	-0.07023	-361.745	-2.24E-06
57-114	8.55452	8.808556	-2.96962	8.554528	-9.43E-05
58-60	-336.355	-335.279	0.319754	-336.292	0.018516
59-116	-1939.82	-1939.82	0	-1939.82	0
60-73	400.576	409.2929	-2.1761	400.5628	0.00328
60-100	-791.588	-763.131	3.594943	-789.53	0.26002
60-107	1258.646	1239.159	1.548242	1258.636	0.000834
60-112	4901.78	4867.614	0.697008	4901.395	0.007849
60-118	2657.141	2595.45	2.321701	2657.355	-0.00806
61-76	545.6312	552.8616	-1.32514	545.6523	-0.00388
61-89	-593.151	-586.169	1.177086	-593.242	-0.0154
61-98	-62.5111	-60.9491	2.498672	-62.5172	-0.00978
61-115	-781.237	-802.984	-2.7836	-781.102	0.017285
62-70	-74.67	-74.67	0	-74.67	0
65-70	-1360.32	-1358.24	0.1529	-1360.39	-0.00497
65-97	-31.825	-19.5543	38.55674	-31.824	0.00323
65-112	-667.783	-683.359	-2.33242	-667.666	0.017544
66-90	-185.798	-185.798	0	-185.798	0
67-120	-12.632	-12.632	0	-12.632	0
68-72	315.3356	313.7487	0.503254	315.3034	0.010215
69-84	6.509	6.509	0	6.509	0
69-114	70.61648	70.36244	0.359741	70.61647	1.14E-05
70-88	0	6.46E-13	0	0	0
70-109	-368.282	-367.655	0.170244	-368.369	-0.02337
70-112	1220.65	1216.079	0.374456	1221.061	-0.03369
71-82	900.0896	896.9557	0.348171	900.1525	-0.00699
72-81	29.95225	30.58256	-2.10439	30.01216	-0.20001
72-82	-174.535	-176.416	-1.07817	-174.854	-0.18294
72-99	-72.5544	-71.9909	0.776758	-72.5784	-0.03301
73-112	144.5221	158.8092	-9.88576	144.484	0.026399
74-112	-557.752	-557.752	0	-557.752	0
75-87	-44.7184	-44.7445	-0.05846	-44.6933	0.056044
75-102	-3.05014	-9.63485	-215.882	-3.03852	0.381017
75-116	-224.596	-216.766	3.486243	-224.659	-0.02802
75-118	-206.363	-207.582	-0.59076	-206.336	0.012724
76-98	-361.135	-353.904	2.00213	-361.114	0.005858
77-89	15.34391	16.29249	-6.18218	15.34355	0.002315
78-103	-24.701	-24.701	0	-24.701	0
79-102	-343.419	-354.807	-3.31616	-343.419	0.000113
81-82	-247.08	-248.802	-0.69676	-247.039	0.016709
85-91	1214.9	1199.901	1.234578	1214.816	0.006894
85-96	48.04569	48.34106	-0.61476	48.05236	-0.01389
86-102	-818.406	-862.297	-5.36296	-818.394	0.001544
86-116	-1406.89	-1330.67	5.417479	-1406.87	0.001171
87-102	32.24577	29.35918	8.951838	32.23161	0.043921
87-116	277.2665	279.5138	-0.81049	277.1224	0.052001
87-118	-1045.02	-1044.4	0.058681	-1044.83	0.017551
89-93	395.18	395.18	0	395.18	0
89-98	192.8037	192.3134	0.254294	193.6259	-0.42646
89-112	-1981.85	-1975.49	0.321056	-1981.82	0.0019
89-115	1436.631	1463.45	-1.86679	1436.385	0.017077

91-104	601.237	601.237	0	601.237	0
94-95	-9.424	-9.424	0	-9.424	1.06E-08
94-120	19.49754	18.45235	5.360593	19.49757	-0.00018
98-115	171.1051	170.9442	0.094016	171.338	-0.13612
100-102	1058.088	1132.099	-6.99478	1058.19	-0.00964
100-116	466.7099	506.0197	-8.42274	466.7506	-0.00872
100-118	1721.607	1705.254	0.949904	1721.188	0.024355
102-116	-38.0896	-32.3974	14.94432	-38.1089	-0.05056
103-119	11.15494	11.19558	-0.36426	11.15494	5.09E-05
105-112	-138.952	-138.952	0	-138.952	0
108-112	-66.058	-66.058	0	-66.058	0
113-116	168.8395	150.5254	10.84703	168.8129	0.015707
116-118	-3496.37	-3412.63	2.395092	-3496.38	-0.00042

Based on Table 6.1, following things are observed:

[1] 0% error is because of the lines radially connected.

[2] Maximum absolute errors:

(a) Ref. [8] : 215.88% (at line 185; corrected reactances yield 0.381% error)

(b) Using CF's: 5.063 % (at line 61; [8] yield 3.143% error)

(Out of 216 lines, 211 lines yield much better answer than [8])

[3] Mean absolute error:

(a) Ref. [8]: 4.8885%

(b) Present method: 0.0614%

The inter-zonal power flow error considering DC_reac and AC_reac is shown in Fig.6.4.

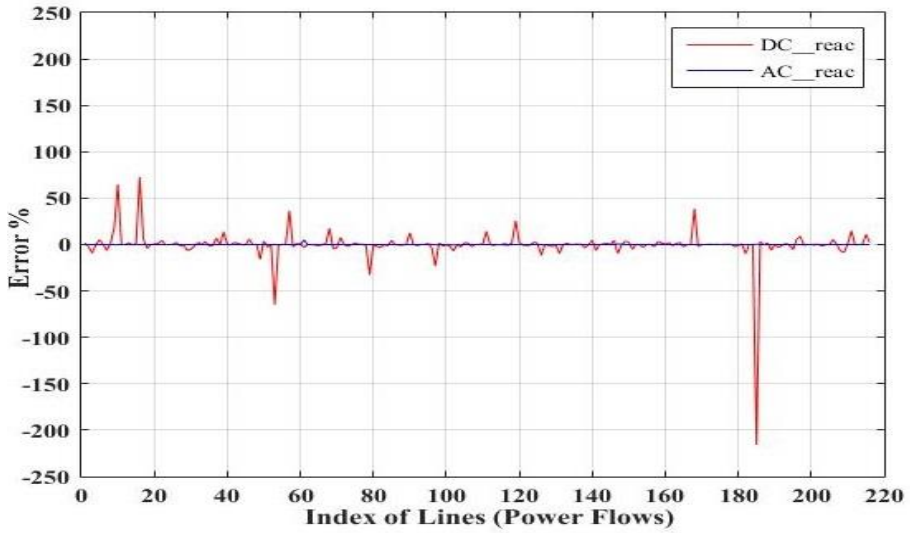

Fig.6.4 Power flow error considering DC_reac and AC_reac at base case

In order to view the robustness of the method, power flows for a non-base case (-10 to 10% change in injected power) is shown in Table 6.2

Table 6.2 Comparison of Power Flows at non-base case (-10% to +10% change)

Lines	Actual Power flow obtained by *NR*	*PTDFr*Pr* [8] 'or' Power flow with *DC_reac*	Error *%*	Power flow with *AC_reac*	Error *%*
1-70	-1691.92	-1639.86	3.08	-1700.52	-0.51
1-109	-1036.89	-1088.96	-5.02	-1028.3	0.83
2-21	190.0199	213.178	-12.19	189.1221	0.47
2-22	-3865.63	-3865.63	0	-3865.63	0
2-60	-1242.09	-1162.73	6.39	-1163.11	6.36
2-92	145.7549	145.7549	0.00	145.7549	0.00
2-110	211.3337	243.9032	-15.41	207.3834	1.87
2-113	1497.577	1472.131	1.70	1481.197	1.09
2-116	435.6187	345.2115	20.75	402.3261	7.64
2-118	33.03314	13.80319	58.21	28.5723	13.5041
3-21	-340.963	-340.963	0	-340.963	0
4-56	1601.796	1601.796	0	1601.796	0
5-14	382.9775	376.2687	1.75	385.0758	-0.55
5-65	-224.637	-221.708	1.30	-251.384	-11.91
5-70	-1495.72	-1492.66	0.20	-1535.13	-2.64
5-89	-80.8646	-73.8004	8.74	-82.7432	-2.323
5-97	143.9321	140.1583	2.62	141.2232	1.88
5-115	-62.4796	-65.0472	-4.11	-63.827	-2.16
6-17	303.2071	303.2071	0	303.2071	0
6-23	399.794	393.1915	1.65	395.587	1.05
6-25	-168.265	-168.699	-0.26	-171.522	-1.94
6-34	-62.3164	-56.4343	9.44	-53.8505	13.59
6-63	195.097	195.097	0	195.0971	0
6-64	-583.657	-583.657	0	-583.657	0
6-90	691.6674	692.8214	-0.17	690.6656	0.14
7-8	-38.4452	-33.491	12.89	-37.5151	2.42
7-58	401.3628	393.3739	1.99	382.1325	4.79
7-60	-926.067	-923.032	0.33	-907.766	1.98
8-58	13.78526	13.25682	3.83	13.26149	3.80
8-60	-448.814	-494.57	-10.19	-464.046	-3.39
8-73	360.3599	358.4411	0.53	354.9696	1.50
8-107	-740.153	-686.996	7.18	-718.077	2.98
9-55	-40.3792	-40.3792	0	-40.3792	0
10-70	-321.029	-307.602	4.18	-311.374	3.01
10-109	-586.412	-599.839	-2.29	-596.067	-1.65
11-12	194.2537	195.6182	-0.70	194.1614	0.05
11-21	29.1553	0.211774	99.27	28.1529	3.44
11-38	217.8128	217.8128	0	217.8128	0
11-50	33.36272	-1.08143	103.24	25.2063	24.45
11-77	344.6957	347.276	-0.75	344.1719	0.15
11-83	77.14883	77.14883	0	77.14883	0
11-112	-97.9039	-38.4611	60.72	-88.129	9.98
12-112	-195.794	-194.43	0.70	-195.887	-0.05
13-36	-260.064	-260.064	0	-260.064	0

14-70	-579.179	-584.774	-0.97	-582.867	-0.64
14-97	75.64334	74.53004	1.47	81.42932	-7.65
15-16	-416.718	-416.718	0	-416.718	0
16-68	2531.832	2531.832	0	2531.832	0
16-79	-53.5148	-63.4571	-18.58	-54.7122	-2.24
16-86	-830.514	-786.673	5.28	-830.612	-0.01
16-100	-2216.19	-2283.11	-3.02	-2228.29	-0.55
16-102	-356.762	-357.945	-0.33	-354.096	0.75
16-116	51.65093	85.85279	-66.22	62.38525	-20.78
18-37	-7.87348	-10.3109	-30.96	-8.1655	-3.71
18-94	-368.172	-363.438	1.29	-369.385	-0.33
18-103	174.5379	172.3499	1.25	176.2069	-0.96
18-119	0.283031	0.17442	38.37	0.1194	57.81
19-32	-107.08	-96.5133	9.87	-106.422	0.62
19-34	343.1011	323.2012	5.80	348.3363	-1.53
19-37	-496.618	-435.631	12.28	-506.097	-1.91
19-39	-44.5733	-25.4312	42.95	-72.7846	-63.29
19-53	1044.653	1002.71	4.02	1045.19	-0.05
19-68	-149.154	-187.309	-25.58	-126.003	15.52
19-71	-314.423	-331.793	-5.52	-316.901	-0.79
19-72	343.5578	368.8664	-7.37	349.85	-1.83
19-82	-599.393	-598.03	0.23	-595.097	0.72
20-27	-165.587	-162.38	1.94	-164.602	0.59
20-30	11.41641	8.210296	28.08	10.43207	8.62
21-50	215.2658	126.4268	41.27	207.2876	3.71
21-58	-185.832	-172.931	6.94	-156.586	15.74
21-110	121.7556	135.6468	-11.41	121.401	0.29
21-111	207.5156	207.5156	0	207.5156	0
21-112	1027.491	1083.753	-5.48	1004.678	2.22
23-41	76.04457	76.04457	0	76.04457	0
23-90	159.6024	152.9999	4.14	155.3955	2.64
24-85	-313.069	-313.069	0	-313.069	0
25-27	302.0687	298.8626	1.06	301.0844	0.33
25-30	79.02382	81.61427	-3.28	80.22802	-1.52
25-34	61.73038	111.283	-80.27	60.07919	2.67
25-37	-577.283	-593.153	-2.75	-566.022	1.95
25-68	-956.9	-979.316	-2.34	-966.028	-0.95
25-90	124.8342	130.2827	-4.36	130.0429	-4.17
25-94	-739.488	-753.536	-1.90	-746.456	-0.94
25-106	55.21026	55.82592	-1.12	54.9904	0.40
25-120	-22.9958	-26.0972	-13.49	-24.9742	-8.60
26-44	-282.383	-282.383	0	-282.383	0
28-36	-184.315	-207.871	-12.78	-192.04	-4.19
28-43	220.7883	244.3436	-10.67	228.5126	-3.50
29-69	170.9505	170.9505	0	170.9505	0
30-106	4.925126	4.309468	12.50	5.144988	-4.46
31-112	-266.37	-266.37	0	-266.37	0
32-71	-111.001	-110.248	0.68	-99.6817	10.20
32-82	738.6582	748.4727	-1.33	727.9982	1.44
33-50	-98.7553	-98.7553	0	-98.7553	0
34-68	-1253.85	-1225.65	2.25	-1254.57	-0.06
34-72	-128.61	-151.738	-17.98	-136.821	-6.39
34-81	-8.40162	-13.7364	-63.50	-10.2997	-22.59

34-82	-529.048	-493.247	6.77	-506.162	4.33
35-44	64.03365	65.01298	-1.53	65.99563	-3.06
35-61	114.711	107.0114	6.71	129.9191	-13.26
35-89	368.1945	373.7105	-1.50	304.9349	17.18
35-98	-119.438	-113.307	5.13	-73.3664	38.57
35-101	252.4617	252.4617	0	252.4617	0
35-115	-104.875	-109.802	-4.70	-104.857	0.02
36-56	-352.848	-395.424	-12.07	-357.589	-1.34
36-85	1482.748	1470.683	0.81	1478.707	0.27
36-91	749.0761	780.1615	-4.15	750.1332	-0.14
37-51	93.70566	94.12803	-0.45	93.5454	0.17
37-52	88.8321	88.53034	0.34	88.24968	0.66
37-68	-375.998	-347.867	7.48	-387.536	-3.07
37-94	5.824548	18.23991	-213.16	15.98506	-174.44
37-99	225.4655	224.4776	0.44	228.9359	-1.54
37-103	67.2081	70.20973	-4.47	67.34776	-0.21
37-117	121.489	121.489	0	121.489	0
39-53	-29.874	12.06876	140.40	-30.4111	-1.80
39-82	-297.494	-320.295	-7.66	-325.169	-9.30
40-60	-218.886	-225.556	-3.05	-217.407	0.68
40-107	-99.3513	-92.6812	6.71	-100.83	-1.49
42-79	12.93807	10.22107	21.00	13.71005	-5.97
42-86	-183.459	-180.742	1.48	-184.231	-0.42
43-55	290.9328	-6.18831	102.13	297.2693	-2.18
43-56	-181.512	43.53438	123.98	-181.681	-0.09
43-60	103.0985	198.7291	-92.76	104.6556	-1.51
44-61	258.9554	233.2147	9.94	262.1077	-1.22
44-89	-742.922	-718.213	3.33	-744.582	-0.22
44-98	-16.6827	-14.6723	12.05	-16.2129	2.82
45-89	-479.155	-479.155	0	-479.155	0
46-48	559.4468	470.7204	15.86	579.5936	-3.60
46-84	-188.4	-184.875	1.87	-186.22	1.16
46-85	-665.213	-578.784	12.99	-683.104	-2.69
46-91	-14.3817	-15.6096	-8.54	-18.8185	-30.85
47-90	-285.27	-285.27	0	-285.27	0
48-70	3361.277	3320.632	1.21	3363.251	-0.06
48-80	423.2952	423.2952	0	423.2952	0
48-84	-1376.76	-1380.28	-0.26	-1378.94	-0.16
48-85	-2893.01	-2984.32	-3.16	-2868.99	0.83
48-96	135.6172	132.5131	2.29	135.4556	0.12
48-109	1000.079	1049.94	-4.99	996.5806	0.35
49-50	73.22264	73.22264	0	73.22264	0
50-110	78.80235	32.34173	58.96	83.10733	-5.46
50-112	140.3207	63.49819	54.75	119.8811	14.57
51-52	34.37744	34.79981	-1.23	34.21718	0.47
52-99	-38.0851	-37.2595	2.17	-37.1828	2.37
52-103	45.40857	44.70351	1.55	43.76357	3.62
54-99	-38.7571	-38.7571	0	-38.7571	0
55-56	-788.145	-852.142	-8.12	-758.074	3.82
55-60	-346.386	-579.219	-67.22	-339.739	1.92
55-100	410.4393	410.1473	0.07	380.0568	7.40
56-60	2277.814	2271.646	0.27	2278.329	-0.02
56-85	253.3177	243.5124	3.87	254.7767	-0.58

56-100	2547.805	2681.175	-5.23	2558.899	-0.44
56-102	872.4764	873.5534	-0.12	884.5703	-1.39
57-69	-381.674	-381.572	0.03	-380.932	0.19
57-114	9.937314	9.835106	1.03	9.195284	7.47
58-60	-356.86	-352.477	1.23	-347.369	2.66
59-116	-2038.26	-2038.26	0	-2038.26	0
60-73	418.7471	429.2721	-2.51	421.6108	-0.68
60-100	-839.333	-772.084	8.01	-758.971	9.57
60-107	1347.308	1287.481	4.44	1326.711	1.53
60-112	5114.515	5053.867	1.19	5152.66	-0.75
60-118	2782.622	2716.302	2.38	2783.589	-0.03
61-76	569.9969	575.8215	-1.02	572.7294	-0.48
61-89	-595.278	-549.08	7.76	-620.489	-4.24
61-98	-62.5559	-64.3406	-2.85	-65.6297	-4.91
61-115	-860.414	-944.093	-9.73	-816.502	5.10
62-70	-79.4856	-79.4856	0.00	-79.4856	0.00
65-70	-1420.22	-1416.82	0.24	-1429.17	-0.63
65-97	-31.9132	-27.0261	15.31	-34.9903	-9.64
65-112	-728.114	-733.467	-0.74	-742.83	-2.02
66-90	-196.694	-196.694	0.00	-196.694	0.00
67-120	-16.2618	-16.2618	0	-16.2618	0
68-72	335.8919	331.6486	1.26	337.6504	-0.52
69-84	7.12849	7.12849	0	7.12849	0
69-114	74.52013	74.62233	-0.14	75.26216	-1.00
70-88	0	0	0	0	0
70-109	-376.536	-360.908	4.15	-371.98	1.21
70-112	1243.976	1254.048	-0.81	1190.393	4.31
71-82	933.8816	917.2642	1.78	942.7216	-0.95
72-81	31.63607	31.95926	-1.02	30.51305	3.55
72-82	-183.557	-186.106	-1.39	-178.222	2.91
72-99	-78.2727	-78.1104	0.21	-82.6454	-5.59
73-112	153.5372	162.1434	-5.61	151.0107	1.65
74-112	-596.022	-596.022	0	-596.022	0
75-87	-47.3313	-46.4925	1.77	-46.8103	1.10
75-102	-0.80278	-13.1364	-1536.36	-2.8063	-249.57
75-116	-243.311	-237.575	2.36	-246.158	-1.17
75-118	-221.645	-215.885	2.60	-217.315	1.95
76-98	-381.822	-375.997	1.53	-379.089	0.72
77-89	17.04567	19.62599	-15.14	16.52186	3.07
78-103	-27.2385	-27.2385	0	-27.2385	0
79-102	-364.778	-377.437	-3.47	-365.203	-0.12
81-82	-257.379	-262.391	-1.95	-260.4	-1.17
85-91	1311.796	1281.938	2.28	1315.176	-0.26
85-96	50.46142	53.5655	-6.15	50.623	-0.32
86-102	-848.911	-901.506	-6.20	-870.563	-2.55
86-116	-1518.91	-1419.76	6.53	-1498.13	1.37
87-102	35.06618	29.51067	15.84	33.90626	3.31
87-116	287.3821	286.9948	0.13	288.5875	-0.42
87-118	-1112.95	-1106.17	0.61	-1112.47	0.04
89-93	419.4025	419.4025	0.00	419.4025	0.00
89-98	190.3638	179.4793	5.72	144.9632	23.85
89-112	-1991.99	-1984.92	0.36	-1925.74	3.33
89-115	1549.531	1639.406	-5.80	1506.148	2.80

91-104	623.3387	623.3387	0.00	623.3387	0.00
94-95	-11.1712	-11.1712	-0.00	-11.1712	-0.00
94-120	19.40704	22.50839	-15.98	21.38539	-10.19
98-115	182.6216	183.9187	-0.71	183.4215	-0.44
100-102	1104.661	1194.72	-8.15	1113.065	-0.76
100-116	473.633	525.3478	-10.92	489.4314	-3.34
100-118	1778.036	1769.671	0.47	1802.802	-1.39
102-116	-42.8194	-36.0104	15.90	-44.8967	-4.85
103-119	10.72829	10.8369	-1.01	10.89192	-1.53
105-112	-144.889	-144.889	0	-144.889	0
108-112	-69.975	-69.975	0	-69.975	0
113-116	190.6934	165.2479	13.34	174.3136	8.59
116-118	-3664.59	-3583.22	2.22	-3670.67	-0.17

The mean absolute error for the non-base case (-10 to +10% change) is:
[i] DC power flow solution **[8] :17.9717**
[ii] Using CF**: 6.1767**
The inter-zonal power flow error considering DC_reac and AC_reac is shown in Fig.6.5.

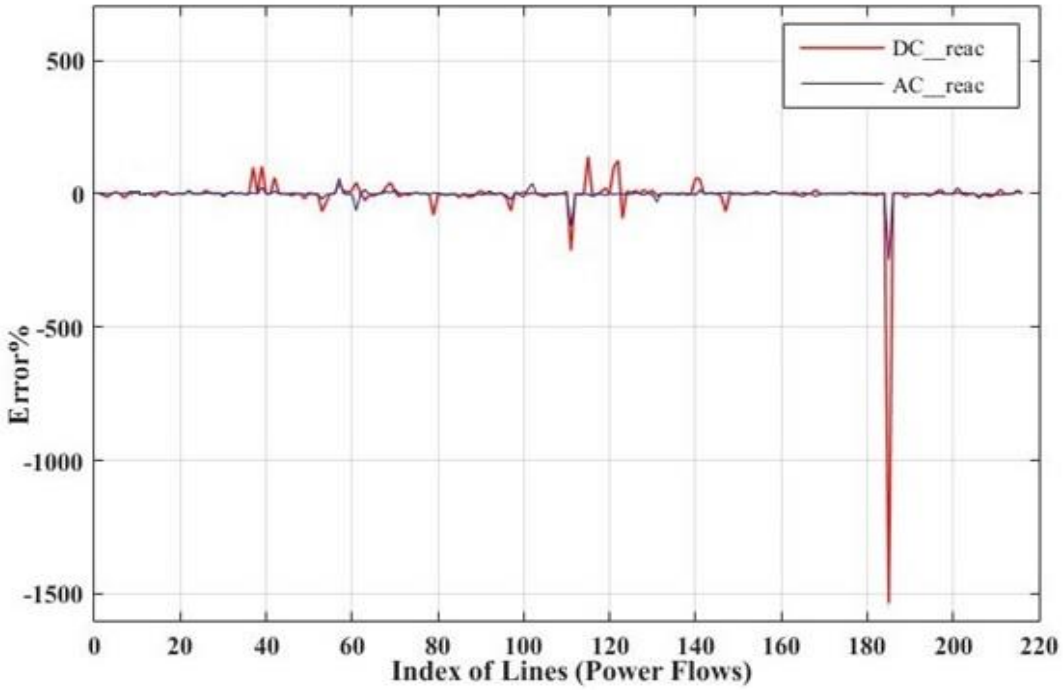

Fig.6.5 Power flow error considering DC_reac and AC_reac at non-base case

CHAPTER 7

CONCLUSION AND FUTURE WORK

7.1 Conclusions

In this report, two network reductions has been performed namely Ward's equivalent and reduction based on PTDF has been carried out and their implementation is also presented in order to show their utility in obtaining a reduced equivalent model of the actual power system. As per the work carried out in this report, the author has reached the following conclusions:

- The PTDF based network reduction technique is more accurate in comparison to other techniques available in literature for obtaining a reduced model which can be formulated either for representing inter-zonal power flows which can be extended for representing power flows in specific lines (having low ATC)
- The PTDF matrix formulation is based on DC-power flow approximations and hence, provides linear power flow solution which is less accurate than empirical solution. By means of a proper factor (known as correction factor), efforts have been made in this report to make use of PTDF matrix and yield a solution closer to an empirical one as compared to any article present in the literature.
- The actual power network should be partitioned in to zones (within which generations and loads are aggregated) by making use of clustering techniques. This will help in aggregating buses having similar sensitivities to power flows in the lines. It has been found in this report that a soft-clustering method (fcm) with induced crispness yields better partitioning as compared to hard clustering (kmeans++).

The ideas developed in this report has been successfully extended to obtain the reduced model of Indian Power System.

7.2 Future Work

Presently, the PTDF matrix is constructed on the basis of DC approximations. One of the approximations is to neglect the line resistances (so that only line reactances are present and system can be considered linear). As a planning tool, PTDF works well, but in an actual scenario, line losses are also present. So, in order to obtain a reduced model which mimics the actual scenario more accurately, line resistances has to be considered. Thus, the challenge will be to have accuracy (considering both line parameters: resistance and reactance) as well as faster performance and simpler calculations (as obtained in a linear system used for DC-flows). If such a reduced model is obtained, then PTDF matrix can also be extended to a distribution system also.

REFERENCES

[1] E. Allen, J. Lang, and M. Ilic, "A Combined Equivalenced Electric, Economic & Market Representation of the Northeastern Power Coordinating Council (NPCC) US Electric Power System," *IEEE Trans. Power Syst.*, vol. 3, no. 3, 2008.

[2] J. Yang, G. Cheng, and Z. Xu, "Dynamic reduction of large power system in PSS/e," *Transmission and Distribution Conference and Exhibition: Asia and Pasific, IEEE/PES,* pp. 1-4, 2005.

[3] J. B. Ward, "Equivalent circuits for power flow studies," *AIEE Trans.Power Appl. Syst.*, vol. 68, pp. 373–382, 1949.

[4] E.C. Housos, G. Irisarri, R.M. Porter, A.M. Sasson, "Steady state network equivalents for Power System planning applications," *IEEE Trans. Power Syst.*, vol. PAS-99, pp. 2113-2120, November 1980.

[5] P. Dimo, *Nodal Analysis of Power Systems*. Kent, U.K.: Abacus, 1975.

[6] X. Cheng and T. J. Overbye, "PTDF-based power system equivalents," *IEEE Trans. Power Syst.*, vol. 20, no. 4, pp. 1868–1876, Nov. 2005.

[7] H. Oh, "A new network reduction methodology for power system planning studies," *IEEE Trans. Power Syst.*, vol. 25, no. 2, pp. 677-684,May 2010.

[8] Di Shi, D.J. Tylavsky, "A Novel Bus-Aggregation based structure-preserving power system equivalent," *IEEE Trans. Power Syst.*, vol.30, no.4, pp. 1977-1986, July 2015.

[9] W. Snyder, "Load-Flow Equivalent Circuits–An Overview," *IEEE PES Winter Meeting*, New York, Jan. 1972.

[10] S. Deckmann, A. Pizzolante, A. Monticelli, B. Stott, and O. Alsac, "Studies on Power System Load Flow Equivalencing," *IEEE Trans. Power App. Syst.*, vol. PAS-99, no.6, pp. 2301–2310, Nov./Dec. 1980.

[11] F.F. Wu and A. Monticelli, "Critical review of external network modelling for online security analysis," *Electrical Power & Energy Systems*, vol.5, no. 4, 1983.

[12] B. Stott, J. Jardim and O. Alsac "DC Power Flow Revisited," *IEEE Transactions on Power Systems*, vol. 24, no. 3, pp. 1290-1300, Aug. 2009

[13] J. M. Undrill and H. H. Happ, "Automatic Sectionalization of Power System Networks for Network Solutions," *IEEE Trans. Power App. and Syst.*, vol. Pas-90, no. 1, Jan./Feb.1971.

[14] M. Ramezani, C. Singh, and M. R. Haghifam, "Role of Clustering in the Probabilistic Evaluation of TTC in Power Systems Including Wind Power Generation," *IEEE Trans. Power Syst.*, vol. 24, no. 2, May 2009.

[15] I. Kamwa, A. K. Pradhan and G. Joos, "Automatic Segmentation of Large Power Systems into Fuzzy Coherent Areas for Dynamic Vulnerability Assessment," *IEEE Trans. Power Syst.*, vol. 22, no. 4, Nov. 2007.

[16] I. Kamwa, A. K. Pradhan, Geza Joos and S. R. Samant, "Fuzzy Partitioning of A Real Power System for Dynamic Vulnerability Assessment," *IEEE Trans. Power Syst.*, vol. 24, no. 3, Aug. 2009.

[17] M. H. Wang and H. C. Chang, "Novel Clustering Method for Coherency Identification using Artificial Neural Network," *IEEE Trans. Power Syst.*, vol. 9, no. 4, Nov. 1994.

[18] H. A. Alsafih, R. Dunn, "Determination of Coherent Clusters in a Multi-machine Power System based on Wide-area Signal Measurements," *IEEE PES General Meeting*, Minneapolis, 2010.

[19] M. H. M. Vale, D. M. FalcBo, and E. Kaszkurewicz, "Electrical Power Network Decomposition for Parallel Computations," *1992 IEEE ISCAS*, vol. 6, pp. 2,761-2,764, San Diego, Calif., May 1992.

[20] G. A. Ezhilarasi and K. S. Swarup, "Network Decomposition using Evolutionary Algorithms in Power Systems," *International Journal of Machine Learning and Computing*, vol. 1, no. 1, April 2011.

[21] S. H. Song, H. C. Lee, Y. T. Yoon and S. I. Moon, "Cluster Design Compatible with Market for Effective Reactive Power Management," *IEEE Power Engineering Society General Meeting*, Montreal, Oct. 2006.

[22] R. Baldick, "Shift factors in ERCOT Congestion Pricing," [Online]. Available: www.ksg.harvard.edu/hepg/Papers/baldick_shift.factors.ercot.cong_3-5-03.pdf. Accessed August 3, 2003.

[23] R. Babuska, Fuzzy Modeling for Control. Boston, MA: Kluwer, 1998.

[24] P. Tan, M. Steinbach, and V. Kumar, *Cluster Analysis: Basic Concepts and Algorithms*.[Online]. Available: http://www-users.cs.umn.edu/~kumar/dmbook/ch8.pdf.

[25] J. C. Bezdek, "Pattern Recognition with Fuzzy Objective Function Algorithms," Plenum, New York (1981).

[26] X. L. Xie and G. Beni, "A validity measure for fuzzy clustering," *IEEE Trans. Pattern Anal. Machine Intell.*, vol. 13, pp. 841-847, Aug. 1991.

[27] N. R. Pal and J. C. Bezdek, "On cluster validity for the fuzzy c-means model," *IEEE Trans. Fuzzy Syst.,* vol. 3, no. 3, pp. 370–379, Aug. 1995

[28] J. Yu, Q. Cheng, and H. Huang, "Analysis of the weighting exponent in the FCM," *IEEE Trans. Syst., Man, Cybern., B, Cybern.*, vol. 34, no. 1, pp. 634–638, Feb. 2004.

[29] J. C. Bezdek, R. J.Hathaway, et al, "Convergence and theory for fuzzy c-means clustering: counterexamples and repairs," *IEEE Trans. Syst Man Cybern.*, vol.17,n.5, pp. 873–877, 1987

[30] pgcil-development-of-transmission-system-in-india-foir-workshop-at-goa-21-10-2013.

[31] POSOCO, Power Grid, CERC.

[32] Power Atlas of India